

Chapter_12
October_11_2016

12.1. Introduction.

In this chapter we examine the repercussions of coupling deformation and mineral reactions in an open flow hydrothermal system. The result is large amplitude oscillations in temperature and fluid pressure which in turn lead to large oscillations in the equilibrium solubility of gold and of vein filling minerals such as quartz and carbonates. We discuss a model for the deposition of gold in such systems and the resultant controls on ore grade.

Many previous workers have recognised episodic behaviour in hydrothermal systems. Examples are crack-seal veins (Cox and Etheridge, 1983; Fisher and Brantley, 1992), laminated quartz veins (Chase, 1949; Vearncombe, 1993), compositional zoning in minerals (Thomas et al., 2011) including gold (Butt and Timms, 2011), multiple overprinting brecciation events (Boullier and Robert, 1992; Oreskes and Einaudi, 1990), and fluid inclusion histories (Wilkinson and Johnson, 1996). Mechanisms for driving such episodic behaviour are commonly proposed to arise from pore fluid pressure fluctuations associated with adiabatic seismic events and associated fault-valve behaviour or suction pump/piston processes (Sibson, 1987, 1995, 2001, Boullier and Robert, 1992; Cox, 1995, 2005; Henley and Berger, 2000; Weatherley and Henley, 2013; Sanchez-Alfaro et al., 2016; Cox, 2016). These mechanisms call for catastrophic fluid depressurisation (Weatherley and Henley, 2013) and resulting adiabatic deposition of gold by phase separation processes (Simmons and Brown, 2006). One might call such mechanisms *extrinsic* since they rely on the activity of processes outside the hydrothermal system associated with crustal scale deformations. In this chapter we emphasise that hydrothermal systems are unstable dynamical systems and that *intrinsic* processes (aseismic chemo-thermal-deformation processes operating entirely within the system) result not only in fluctuations in pore pressure but also in large excursions in temperature with resultant influences on localised gold deposition. These events are orders of magnitude slower than seismic events and probably overlap the time scales for slow earthquakes. The resulting pore pressure drops are non-adiabatic and are associated with large temperature drops. Some aspects of intrinsic episodic processes have been considered by Henley and Berger (2000).

Since hydrothermal systems evolve both spatially and temporally they are dynamical systems and since they are open to the input of fluids, heat and chemical components they are non-equilibrium dynamical systems. The processes that operate within these systems are nonlinear and inter-related; examples are the exponential dependence of reaction rates on temperature, dependence of the activation energy of a reaction on pH, the competition between diffusion of fluids to or away from reaction sites and the production of fluid at a devolatilising site, and the production of heat from brecciation and exothermic chemical reactions and its coupling to fluid pressure and chemical reaction rates. Thus hydrothermal mineralising systems are nonlinear, non-equilibrium dynamical systems and in this chapter we consider some aspects of the nonlinear dynamics of such systems.

Mineralising hydrothermal systems associated with orogenic gold deposits evolve with time. Two modes of operation can be distinguished. The first is an exothermic, fluid absorbing phase with the pervasive development of hydrous silicates such as sericite and chlorite and of carbonates such as calcite, ankerite and siderite from anhydrous phases such

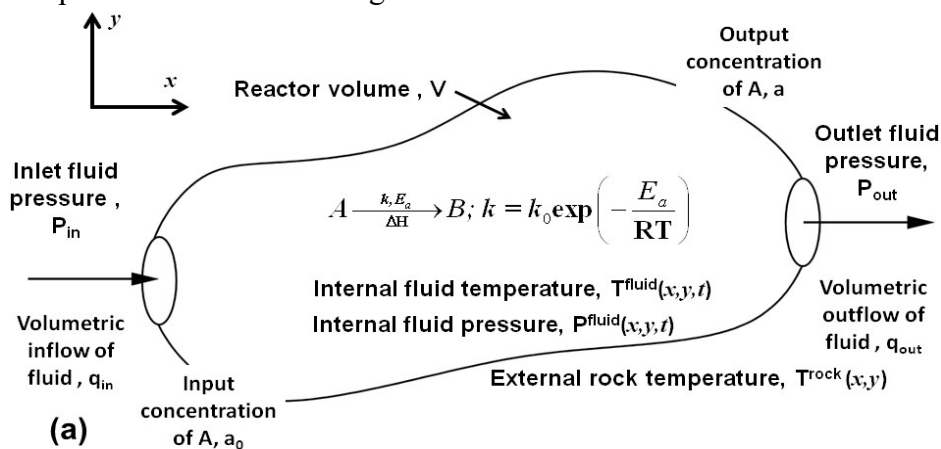
45 as pyroxenes and feldspars. This stage may or may not be associated with weak
 46 mineralisation. The second mode is more localised and typically higher in temperature than
 47 mode I. Mode II is characterised by competition between exothermic processes (such as
 48 fracturing, brecciation, stock-work formation and veining) and endothermic processes such as
 49 dehydration or decarbonisation of previously formed alteration assemblages, and the
 50 deposition of metals such as gold. Anhydrous silicates such as epidote or K-feldspar may
 51 form at this stage and typically the processes release fluids previously bound in hydrous or
 52 carbonate alteration assemblages during mode I. Mode II is noticeably episodic with many
 53 (100's to 1000's) overprinting events recorded as multiple stages of brecciation, crack-seal
 54 microstructures, laminated veins, compositional zoning in minerals, fluid inclusion
 55 compositions and multiple stages of gold deposition, and sometimes, gold dissolution
 56 (Cameron, 1998) and remobilisation (Fougerouse et al., 2016). For examples of these modes
 57 of operation in hydrothermal systems see Oreskes and Einaudi (1990), Wilkinson and
 58 Johnson (1996), Barnicoat et al. (1997), Henley and Berger (2000), Baker et al. (2103),
 59 Wilson et al. (2009, 2013), Schaubs and Zhao (2002), and Zhu et al. (2011).

60 12.2. Orogenic gold systems as open flow chemical reactors.

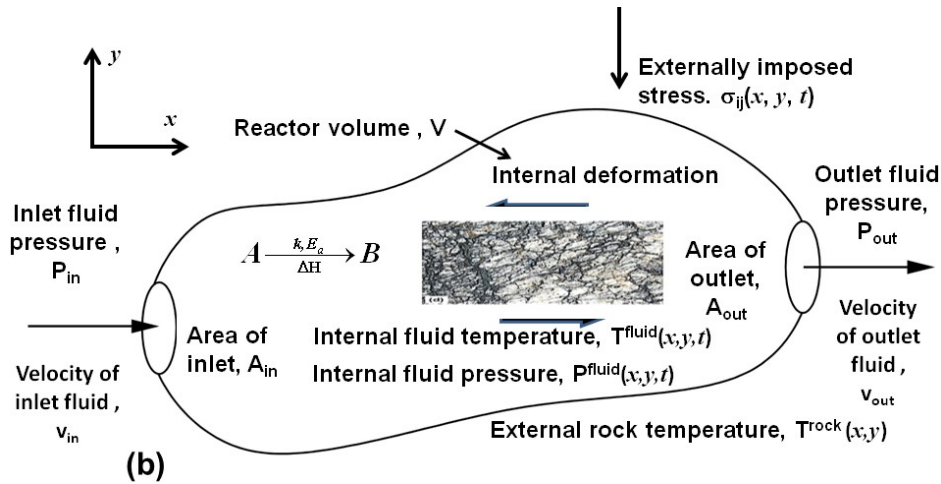
61 The essential ingredient for the formation of an orogenic gold hydrothermal system is
 62 the influx of hot fluids bearing chemical components such as CO₂, H⁺, H₂S and Au. The
 63 distribution of such fluids within the system is influenced by local variations in fluid pressure
 64 which arise from the distributions of temperature, permeability and of mechanical and
 65 chemical dilatancy. The flow itself adds energy to the system in the form of heat and
 66 momentum and creates the chemical environment for alteration and mineralising reactions to
 67 proceed. Since the mineral reaction rates are a sensitive function of fluid supply the spatial
 68 distribution of fluid flow rates becomes a critical issue for the development of the system. In
 69 this section we consider some aspects of open flow systems, in particular, the control of
 70 mineral reaction rates by the supply of fluids and heat together with controls on the
 71 equilibrium solubilities of gold and quartz and on the deposition of gold and quartz.

72 12.2.1. The models considered in this chapter.

73 In order to emphasise the essential features of orogenic gold hydrothermal systems we
 74 idealise the processes involved in Figure 12.1.



75



76
77

78 Figure 12.1. The two idealised end-member hydrothermal systems considered in this chapter. The systems are
79 open flow chemical reactors with volume, V . The inlet and outlet areas of the system are A_{in} and A_{out} with inlet
80 and outlet fluid flow velocities v_{in} and v_{out} . This means we can define inlet and outlet fluid fluxes as $q_{in} = v_{in}/A_{in}$
81 and $q_{out} = v_{out}/A_{out}$. The inlet fluid pressure is P_{in} . Darcy's law, the value of q_{in} and the presence of internal
82 sources and sinks of fluids then establish the local fluid pressure, P^{fluid} , as a function of the spatial coordinates, x ,
83 y and of time, t . These relationships then establish the outlet fluid pressure and fluid velocity, P_{out} and v_{out} .
84 Mineral reactions occur within the reactor one of which is $A \xrightarrow[k, E_a]{\Delta H} B$ with rate constant, k , and enthalpy of

85 reaction, ΔH . In general k depends on the absolute temperature, T , through $k = k_0 \exp\left(-\frac{E_a}{RT}\right)$ where k_0 is a

86 reference rate, E_a is the activation energy and R is the gas constant. This reaction also has an associated volume
87 change, ΔV and may or may not produce fluids. The external rock temperature is T^{rock} which is a function of x
88 and y . Internal deformation occurs under the influence of externally imposed stresses, σ_{ij} , also a function of x , y
89 and t . Heat liberated from these deformations and from chemical reactions combines with the temperature of the
90 incoming fluid and diffusion of heat through and from the system to produce an internal temperature
91 distribution, $T^{fluid}(x, y, t)$. Fluctuations in temperature combined with episodic release of fluid from mineral
92 reactions also lead to fluctuations in fluid pressure, $P^{fluid}(x, y, t)$. (a) A system that is not deforming with a single
93 exothermic mineral reaction that does not produce fluids. (b) A deforming system in which the deformation
94 (brecciation and fracturing) is exothermic, coupled to a mineral reaction that may be endothermic and producing
95 fluids. Figures modified substantially from Rawlings and Ekerdt (2013, Figure 6.2).

96 We consider an open flow system (Figure 12.1) which comprises a chemical reactor
97 with volume, V . The inlet and outlet areas of the system are A_{in} and A_{out} with inlet and outlet
98 fluid flow velocities v_{in} and v_{out} . Thus the inlet and outlet fluid fluxes (with units $m^3 s^{-1} m^{-2}$)
99 are $q_{in} = v_{in}/A_{in}$ and $q_{out} = v_{out}/A_{out}$. The inlet fluid pressure is P_{in} . Darcy's law, the value of q_{in}
100 and the presence of internal sources and sinks of fluids then establishes the local fluid
101 pressure, P^{fluid} , and gradients in P^{fluid} as a function of the coordinates, x , y and of time, t ,
102 together with the outlet fluid pressure and fluid velocity, P_{out} and v_{out} . Mineral reactions occur
103 within the reactor, one of which is $A \xrightarrow[k, E_a]{\Delta H} B$ with rate constant, k , and enthalpy of reaction,

104 ΔH ; k depends on temperature through an Arrhenius relation, $k = k_0 \exp\left(-\frac{E_a}{RT}\right)$, where E_a is

105 the activation energy for the reaction, R is the gas constant and k_0 is a reference rate. Some
106 reactions are endothermic and remove heat from the system and some are exothermic and add
107 heat to the system. These reactions also have an associated volume change, ΔV and may or

108 may not produce fluids. Reactions that produce hydrous or carbonate silicates from
 109 anhydrous or un-carbonated silicates remove fluids from the system. Reactions that produce
 110 anhydrous silicates from hydrous assemblages add fluids back into the system. The external
 111 rock temperature is T^{rock} which is a function of x and y . Internal deformation occurs under the
 112 influence of externally imposed stresses, σ_{ij} , also a function of x , y and t . Heat liberated from
 113 these deformations and from chemical reactions combines with the temperature of the
 114 incoming fluid and diffusion of heat through and from the system to produce an internal
 115 temperature distribution that is a function of both space and time, $T^{\text{fluid}}(x, y, t)$. Fluctuations in
 116 temperature combined with episodic release of fluid from mineral reactions also lead to
 117 temporal and spatial fluctuations in fluid pressure, $P^{\text{fluid}}(x, y, t)$. The energy balance of the
 118 system is given by

$$\begin{aligned}
 \left[\begin{array}{l} \text{Rate of energy} \\ \text{accumulation} \end{array} \right] &= \left[\begin{array}{l} \text{Rate of energy} \\ \text{entering system} \\ \text{by inflow} \end{array} \right] - \left[\begin{array}{l} \text{Rate of energy} \\ \text{leaving system} \\ \text{by outflow} \end{array} \right] \\
 &+ \left[\begin{array}{l} \text{Rate of heat added to or removed} \\ \text{from the system by diffusion} \end{array} \right] + \left[\begin{array}{l} \text{Rate of work} \\ \text{done on and in the system by} \\ \text{internal deformation} \end{array} \right] \\
 &+ \left[\begin{array}{l} \text{Rate of heat added to or removed} \\ \text{from the system by internal mineral reactions} \end{array} \right]
 \end{aligned}
 \tag{12.1}$$

120
 121 A fundamental assumption is that the time scale for the operation of these systems is
 122 less than ≈ 1 million years (see Chapters 2 and 8) so that the rates of heat production from
 123 exothermic mineral reactions and from deformation exceed background crustal radiogenic
 124 heat production rates. Later in this chapter we examine aspects of the energy balance in
 125 (12.1) and show that, in general, the system is unstable and oscillates indefinitely as long as
 126 energy is added to the system and suitable reactants exist within the system. Initially
 127 however, since the mineral reaction rates are sensitively dependent on the supply of fluids
 128 and heat, we need to clarify the influence of such supply issues on the rates of mineral
 129 reactions.

130 **12.3. Principles involved in coupling of processes in hydrothermal systems.**

131 **12.3.1. The coupling between the supply of heat and nutrients to mineral reaction rates.**

132 In Chapter 8 we showed that the behaviour of open flow chemically reacting systems
 133 is intrinsically different to that of thermodynamically closed systems. In closed systems the
 134 kinetics of a chemical reaction depends solely upon the rate constants for the reaction and the
 135 system must ultimately monotonically approach equilibrium. In open systems the rate
 136 constants also play a role in defining the kinetics but the rate of a chemical reaction also
 137 depends on the rates of supply (and removal) of heat and nutrients for the reaction. If the
 138 reaction rate outstrips the net supply of either heat or mass then the reaction stops until the
 139 supply can build up again.

140 Thus, open system behaviour is typically episodic and the system remains far from
 141 equilibrium for as long as energy and mass are added to the system. Multiple non-equilibrium
 142 stationary states can exist, some of which are stable and others unstable. The system can
 143 switch from one stationary state to another or evolve from one state to another depending on
 144 the supply of energy and mass. The episodic behaviour of chemical reactions is characterised
 145 by an *ignition temperature* where the reaction rates become significant and an *extinction*
 146 *temperature* where the reaction rates become insignificant. These temperatures for a
 147 particular reaction depend on the activation energy for that reaction. In fact the paragenetic
 148 sequence in a particular hydrothermal system is a reflection of the sequence of ignition and
 149 extinction temperatures for the particular reactions that produced the paragenetic sequence. In
 150 the models developed in this chapter we consider several examples where the ignition and
 151 extinction temperatures are prescribed.

152 12.2.2. Influence of temperature on fluid pressure.

153 Changes in temperature influence the fluid pressure in the system. In general the rate
 154 of fluid pressure change with time is given by

$$\begin{aligned}
 \left[\begin{array}{l} \text{Rate of change} \\ \text{of fluid pressure} \end{array} \right] &= \left[\begin{array}{l} [1] \text{Rate of fluid pressure change} \\ \text{arising from diffusion of} \\ \text{fluid pressure} \end{array} \right] + \left[\begin{array}{l} [2] \text{Rate of fluid pressure change} \\ \text{arising from temperature change} \end{array} \right] \\
 &+ \left[\begin{array}{l} [3] \text{Rate of fluid pressure change} \\ \text{arising from supply of fluid} \\ \text{from outside the system} \end{array} \right] + \left[\begin{array}{l} [4] \text{Rate of fluid pressure change} \\ \text{arising from devolatilisation; that is,} \\ \text{fluid supply from within the system} \end{array} \right]
 \end{aligned}$$

156 This is a form of reaction-diffusion-advection equation where the diffusion term is
 157 [1], the advection term is [3] and the supply terms are [2] and [4]. Hence we expect this
 158 expression to behave in many different ways both spatially and temporally depending on
 159 competition between diffusion of pressure and generation of pressure. In the early stages of a
 160 hydrothermal system reactions that produce fluid are rare so that the term [4] is not important.
 161 This is the situation we first explore in the next section. Later in the history of the system this
 162 term becomes important and this case is explored as three other models in the next section.

164 Many mineral reactions also involve large volume changes so that pore pressure
 165 changes arise from chemical dilatancy. As an example consider the reaction



167 This reaction results in a volume increase, $\Delta V = +36.7\%$. However if SiO_2 is removed in
 168 solution this results in a volume decrease, $\Delta V = -8.7\%$. If CaCO_3 is also removed then the
 169 total volume decrease is $\Delta V = -42.2\%$. Important questions are: *How are these volume*
 170 *changes expressed in the rock microstructure and what is the influence of such volume*
 171 *changes on fluid pressure and hence on fluid flow and gold solubility?* The answers to these
 172 questions are considered in the remainder of this chapter and in Chapter 8.

173 The influence of temperature on fluid pressure is expressed as (Sulem et al., 2011)

$$174 \quad \frac{\partial P^{fluid}}{\partial t} = \kappa^{fluid} \frac{\partial^2 P^{fluid}}{\partial x_i^2} + \Lambda \frac{\partial T}{\partial t} - K \frac{\partial \phi^{plastic}}{\partial t}$$

175 where κ^{fluid} is the hydraulic diffusivity, $\Lambda = K\phi(\lambda^{fluid} - \lambda^{pore_volume})$ is the undrained pore fluid
 176 thermal expansion coefficient, λ^{fluid} and λ^{pore_volume} are the thermal expansion coefficients of
 177 the pore fluid and of the pore volume, ϕ is the porosity and $\phi^{plastic}$ is the porosity induced by
 178 plastic deformation, K is the elastic bulk modulus of the dry porous solid and we have
 179 assumed the solid matrix is incompressible relative to the compressibility of the fluid.

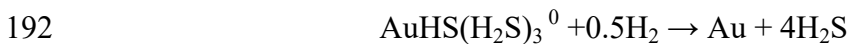
180 In a situation with no deformation, $\frac{\partial\phi^{plastic}}{\partial t} = 0$ but if fracturing or brecciation occurs

181 this term becomes important. The pore fluid thermal expansion coefficient, Λ , depends on the
 182 rock type, effective stress and temperature (Ghabezloo and Sulem, 2009) and varies between
 183 about 0.1 and 0.9 MPa K⁻¹; we assume here a constant value of 0.5 MPa K⁻¹. Thus a 100°C
 184 rise in temperature is equivalent to a pore pressure rise of 50 MPa. Such large changes in pore
 185 pressure can contribute to the formation of veins and breccias if the pore pressure rise is such
 186 that the yield surface is reached.

187

188 12.2.3 Equilibrium solubility of gold and quartz.

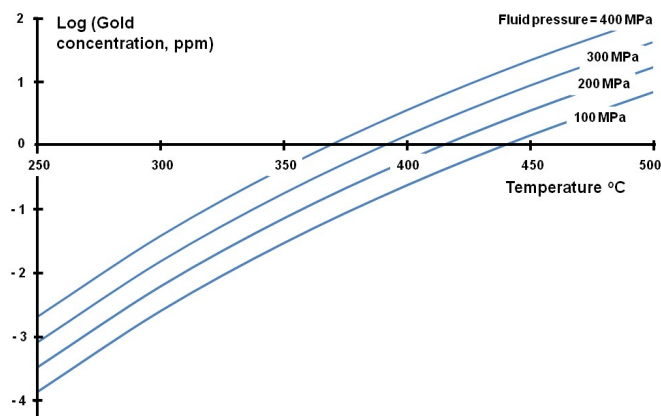
189 Finally we want to model the effect of changes in temperature and fluid pressure on
 190 the solubility of gold and quartz. We take the data of Loucks and Mavrogenes (1999) and
 191 consider the reaction



193 This reaction is endothermic with $\Delta_r H_{T_0}^0 = 105.353 \pm 2.361$ KJ. A fit (Figure 12.2) to the
 194 data of Loucks and Mavrogenes (1999) for the equilibrium solubility of gold, c^{gold} in parts per
 195 million by weight, as the complex $\text{AuHS}(\text{H}_2\text{S})_3^0$ for temperatures between 250°C and 500°C
 196 and pressures between 50 MPa and 400 MPa is given by

197
$$\log c^{gold} = \left[\frac{P^{fluid} + 12.665 \times 10^8}{2.556 \times 10^8} + 5.2769 \right] - \frac{7.572 \times 10^3}{T + 273}$$

198 where P^{fluid} is in Pascals and T is in degrees Centigrade.



199

200 Figure 12.2. Equilibrium solubility of gold as the complex $\text{AuHS}(\text{H}_2\text{S})_3^0$ in ppm by weight of fluid. Modified
 201 from data given by Loucks and Mavrogenes (1999).

202 If we take the densities of rock and of water as 2700 kg m⁻³ and 1000 kg m⁻³
 203 respectively with a rock porosity of 0.1 then a concentration of 1 gram of gold per tonne of
 204 water in the pores of the rock is equivalent to 3.7×10^{-2} ppm of gold by weight of rock.

205 For quartz, the equilibrium solubility of H_4SiO_4 , $m^{equilibrium}$, with units, $mol_{SiO_2}kg_{H_2O}^{-1}$,
 206 as a function of temperature and fluid pressure is taken from Manning (1994):

$$207 \quad \log m^{equilibrium} = A + B \log V + C(\log V)^2$$

208 where $A = -4.66206 + 0.0034063T + 2179.7T^{-1} - 1.1292 \times 106T^{-2} + 1.3543 \times 1087T^{-3}$, $B =$
 209 $-0.00147180T - 806.97T^{-1}$, $C = 3.9465 \times 10^{-4}T$, V (P^{fluid} , T) ($cm^3 g^{-1}$) is the specific
 210 volume of water and in this case T is the absolute temperature. The specific volume of water
 211 over the temperature and fluid pressure ranges of interest is given by Holland and Powell
 212 (1991) and we use that approach here following Ord and Henley (1997).

213 **12.3. Model behaviour.**

214 To illustrate the behaviour of the systems depicted in Figure 12.1 we adopt a model
 215 20 km long and 10 km thick with an embedded reaction system 1 km long and 100 m thick
 216 (Figure 12.3 top). We consider four situations. The first (equivalent to Figure 12.1 a) involves
 217 exothermic alteration reactions where initial silicates are altered to hydrous phases and
 218 carbonates as fluid is added to the system; no fluid is produced during these reactions and no
 219 deformation occurs. The following three situations (equivalent to Figure 12.1 b) involve
 220 deformation of the previously altered system with new reactions that tend to devolatilise the
 221 previously formed assemblage so that fluid is produced internally within the system as fluid
 222 is simultaneously added to the system. In these models the ambient temperature is higher in
 223 the third and fourth examples than in the second. The alteration reactions are endothermic.
 224 The permeability of the model is $10^{-16} m^2$ with $10^{-15} m^2$ for the reaction region; the thermal
 225 conductivity is $2.25 Wm^{-1}K^{-1}$. In model four we decrease the permeability of the country
 226 rock to $10^{-20} m^2$ and the thermal conductivity of the country rock to $2.0 Wm^{-1}K^{-1}$. The
 227 alteration reactions are assumed to follow the type of kinetics shown in Figure 8.11 (b) and
 228 discussed in Section 12.2.1.

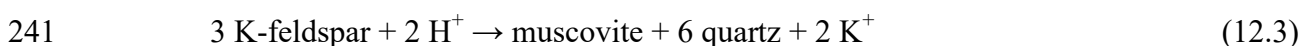
230 **12.3.1. Exothermic reactions with no fluid production and no deformation.**

231
 232 For the model situation shown in Figure 12.1 (a) we suppose that the extinction
 233 temperature for the reaction is $255^\circ C$ with an ignition temperature of $300^\circ C$. Whilst the
 234 reactions are taking place they liberate heat at a rate of $10^{-1} Wm^{-3}$. No fluid is produced
 235 during the reaction. The initial fluid pore pressure is $3.5 \times 10^8 Pa$ (corresponding to a
 236 lithostatic pressure at $\approx 13 km$ depth) and the initial temperature is $250^\circ C$. Other parameters
 237 for the model are given in the caption to Figure 12.1.

238 The types of reactions taking place are represented by reactions such as those below.



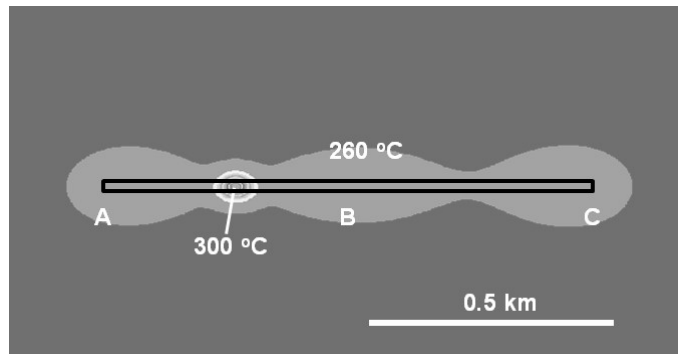
$$240 \quad \Delta H = -783.36 \text{ KJ}$$



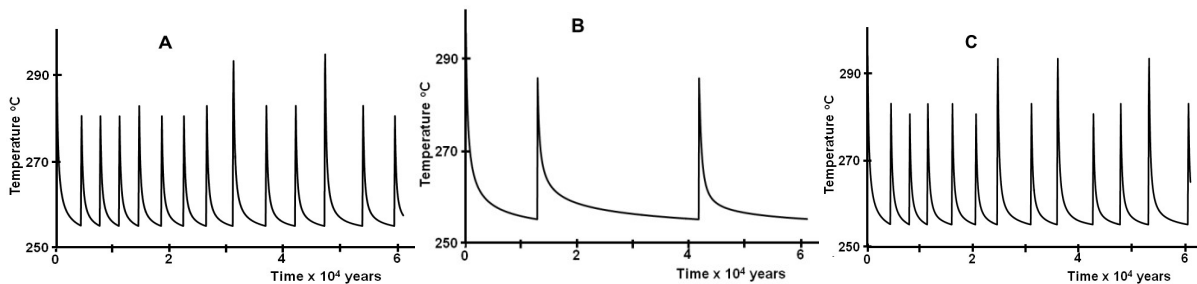
$$242 \quad \Delta H = -485.23 \text{ KJ}$$

243 If we consider reaction (12.2) as an example then 558.7 g of diopside plus anorthite
 244 react to produce 783.36 KJ of heat. Assuming a rock density of $2700 kg m^{-3}$, this is equivalent
 245 to a heat production of $3.79 \times 10^6 Jm^{-3}$ of rock. Thus the value of $10^{-1} Wm^{-3}$ assumed in the

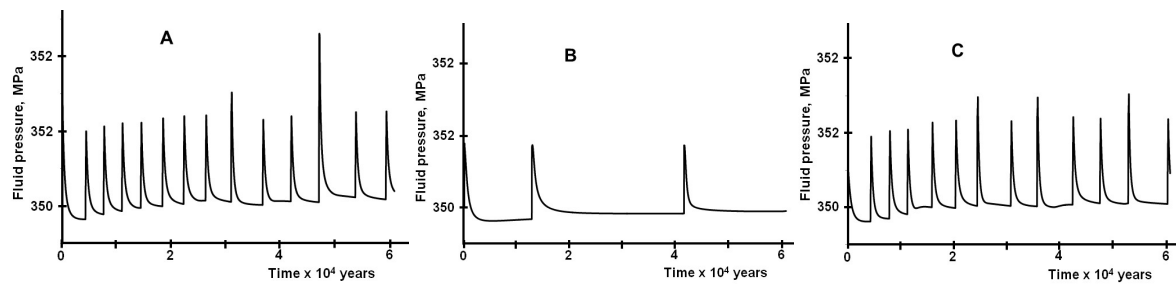
246 modelling is equivalent to the alteration of ≈ 1 cubic metre of rock consisting of diopside and
247 anorthite per 1000 years.



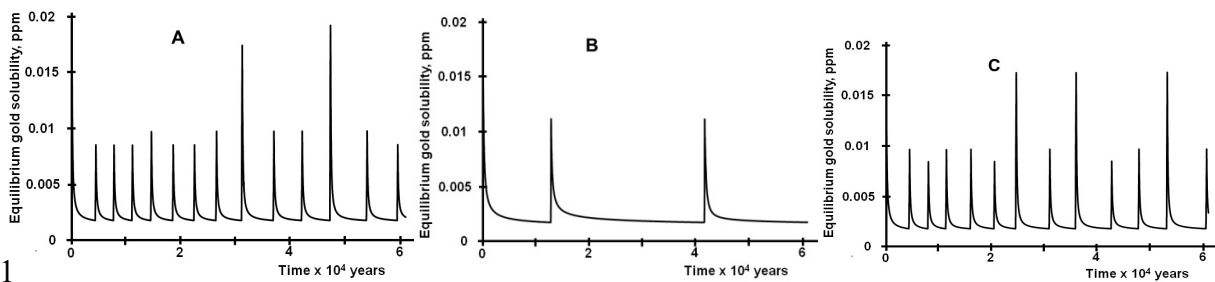
248



249



250



251

252 Figure 12.3. Episodic behaviour in a system involving one exothermic reaction and no deformation (Figure 12.1
253 a) with kinetics given in Figure 8.11 (b). No fluids are released in the reaction and there is no deformation. Top
254 shows the temperature distribution at an instant after 60,000 years. A, B, C are localities where histories are
255 recorded in panels below. First row shows temperature histories at A, B, C. Middle row shows fluid pressure
256 histories at A, B, C. Lower row shows equilibrium gold solubility histories at A, B, C.

257 Figure 12.3 shows the histories of temperature, fluid pressure and equilibrium gold
258 solubility at three points in the hydrothermal system over a period of 60,000 years. At the ends
259 of the system the oscillations have a period of $\approx 4,500$ to $5,000$ years whilst in the central
260 regions the oscillations occur every $\approx 30,000$ years with a reduced maximum amplitude. The
261 period of thermal fluctuations is governed by the rates at which temperature can rise and fall
262 which are functions of the temperature difference between the system and the country rocks,
263 the thermal conductivity of the country rocks and the temperature distribution in immediately

264 adjacent elements of the system. The behaviour overall as shown at an instant in the top frame
265 of Figure 12.3 is spatially quite localised. In most regions the temperature sometimes does not
266 reach the ignition temperature before falling again to the extinction temperature. These spatial
267 and temporal characteristics of the temperature behaviour arise from competition between heat
268 production from the exothermic reaction at a site and conduction of heat away or to that site
269 from adjacent sites.

270 The fluid pressure and equilibrium gold solubility histories mimic the temperature
271 history since they depend only on the temperature. The magnitude of the fluid pressure is a
272 function of competition between thermal expansion of the fluid due to a temperature change
273 and the rate at which fluid pressure can diffuse from the site. Such competitive effects
274 involving diffusion lead to the chaotic spatio-temporal behaviour observed. Although the fluid
275 pressure fluctuations are small they are still sufficient to result in episodic mechanical failure if
276 the stress state is initially close to failure.

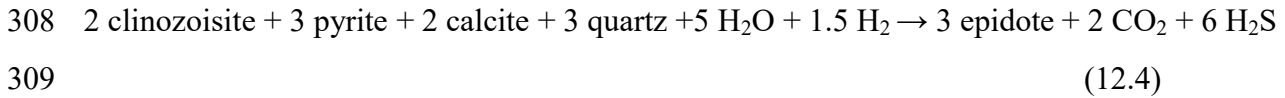
277 The equilibrium gold solubility in this example, although episodic, remains small at \leq
278 0.02 ppm by weight in the fluid, consistent with the small maximum values of temperature and
279 fluid pressure. These values of gold solubility are less than the value of 0.2 ppm by weight in
280 the fluid proposed by Loucks and Mavrogenes (1999) as a possible maximum for gold
281 solubility carried by an entrance fluid. Hence the fluid in this system is always saturated with
282 gold and each temperature-fluid pressure drop means that gold is deposited as a solid. If the
283 rate constant for gold deposition is much greater than the rate constant for gold dissolution then
284 solid gold will slowly accumulate. At the ends of the system shown in Figure 12.3 the total
285 gold accumulated is $\approx 1.85 \times 10^{-4}$ ppm by weight of rock after 60,000 years or 1.4×10^{-3} ppm
286 after 500,000 years. Thus the grades of gold remain low but localised because of the
287 competitive processes mentioned above and the low maximum values of temperature and fluid
288 pressure. Such a hydrothermal system, although strongly altered, would be classified as a
289 failed mineralising system.

290 Of importance in understanding paragenetic sequences is that reactions such as (12.2)
291 imply the episodic deposition of chlorite, quartz and calcite synchronous with the deposition of
292 gold. Reactions such as (12.3) imply fluctuations in pH. These fluctuations do not require
293 autocatalytic reactions although such reactions provide another way of generating episodic
294 fluctuations in pH (Henley and Berger, 2000).

295 **12.3.2. Coupling between deformation and endothermic mineral reactions.**

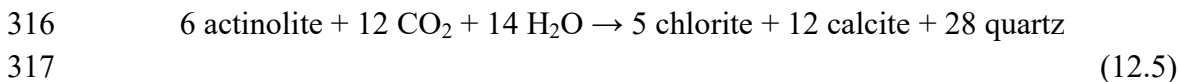
296 Mineralising events (such as deposition of gold) generally overprint the primary
297 alteration assemblages and thus occur later in the history of the system. These mineralising
298 reactions are endothermic and hence enhance the cooling rates of the system. On the other
299 hand, deformation events such as brecciation that are commonly associated with gold
300 deposition are exothermic (Wu et al., 2006). The full coupling between deformation and
301 mineralisation processes has not yet been studied in detail but some relevant results are
302 reported in Alevizos et al. (2014), Veveakis et al. (2014, 2016) and Poulet et al. (2014) with
303 reference to slow earthquakes. Evidently, as the temperature rises during these alteration
304 reactions, endothermic reactions involving devolatilisation of previously formed alteration
305 assemblages and the development of anhydrous silicates such as epidote are initiated by the

306 higher temperatures and in so doing sap heat produced by deformation from the system. A
 307 typical reaction is



310 This reaction is endothermic with $\Delta H = 5937.5 \text{ KJ}$. Thus 1649.2 g of solids on the left
 311 hand side of the reaction are altered to absorb $5.94 \times 10^6 \text{ Joules}$ of heat. This corresponds to
 312 $9.74 \times 10^8 \text{ J m}^{-3}$ if we take the densities of the solids on the left hand side of the reaction to be
 313 2700 kg m^{-3} . Thus 1 cubic metre of rock reacting in 1000 years represents an absorption rate of
 314 0.03 W.

315 For the reaction

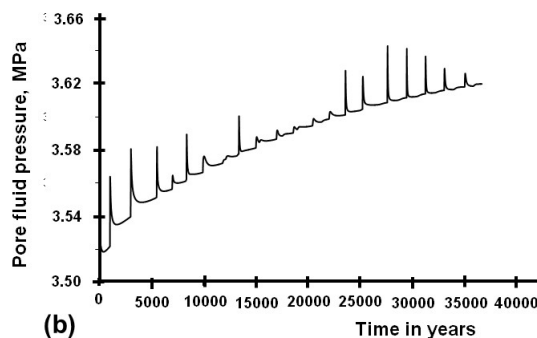
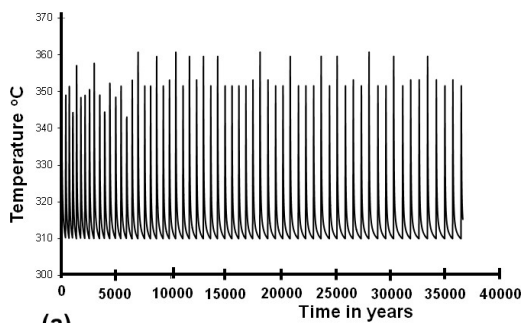


318 $\Delta H = +13409.93 \text{ KJ}$. Thus 5823 g of solids on the left hand side of the reaction are altered to
 319 absorb $13.4 \times 10^6 \text{ Joules}$ of heat. This corresponds to $6.22 \times 10^9 \text{ J m}^{-3}$ if we take the densities
 320 of the solids on the left hand side of the reaction to be 2700 kg m^{-3} . Thus 1 cubic metre of
 321 rock reacting in 1000 years represents an absorption rate of 0.197 W.

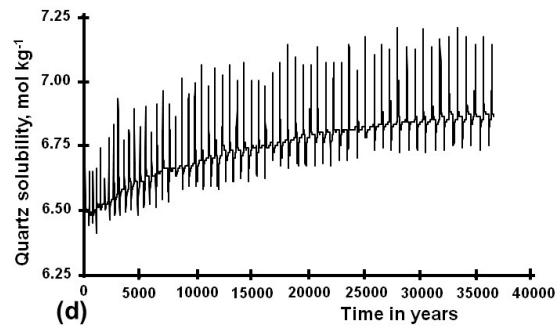
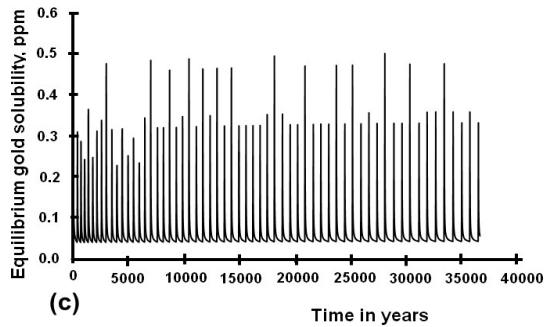
322 We now investigate a model with the same geometry as in Figure 12.3 but with an
 323 endothermic reaction coupled to heat generated by plastic deformation given by

$$324 \quad \dot{H}^{deformation} = \beta \sigma_{ij} \dot{\epsilon}_{ij}$$

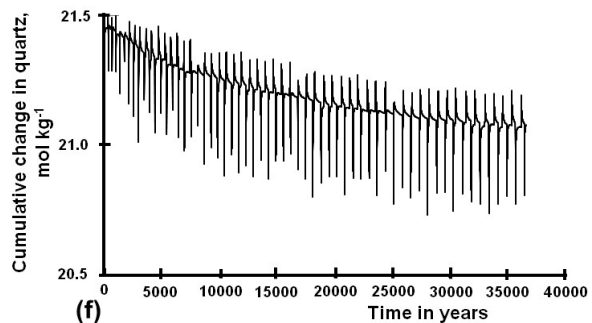
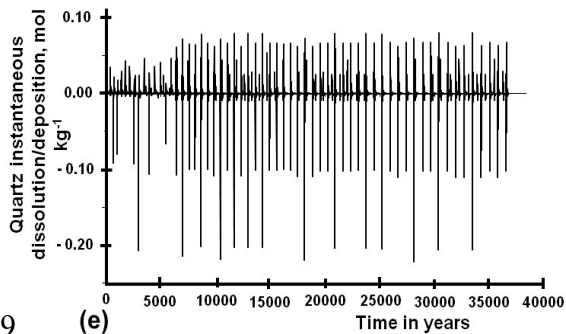
325 where β is the Taylor-Quinney coefficient that measures the amount of heat stored in the
 326 material; σ_{ij} is the stress and $\dot{\epsilon}_{ij}$ is the plastic strain rate. We assume $\beta = 1$ and that the
 327 deformation rate is independent of temperature. For a stress of 100 MPa and a strain rate of 10^{-9} s^{-1}
 328 the heat generated by plastic deformation is 10^{-1} W m^{-3} . We assume that whilst an
 329 endothermic reaction is proceeding, the heat absorption rate for the reaction is 10^{-1} W m^{-3}
 330 which corresponds to a reaction such as (12.5) consuming 1 m^3 of rock every 10^3 years. The
 331 system also differs from that shown in Figure 12.3 in that fluids are released during the
 332 reaction. If we assume that one cubic meter of rock (with density 2700 kg m^{-3}) is altered per
 333 year and releases 1% of its weight as water then this is equivalent to $8.5 \times 10^{-10} \text{ m}^3$ of water per
 334 second. In the models presented here we assume a release rate of $10^{-10} \text{ m}^3 \text{ s}^{-1}$ which is a slow
 335 reaction rate of 1 m^3 of rock, via reactions such as (12.4), every ≈ 10 years. In this model we
 336 also show the history of quartz dissolution/precipitation.



338



339



340

341 Figure 12.4. Episodic behaviour in a relatively low temperature system involving deformation and one
 342 endothermic reaction (Figure 12.1 b) with kinetics given in Figure 8.11 (b). Fluids are released in the reaction.
 343 The geometry is as shown in Figure 12.3 top. Each history is at A in Figure 12.3 top over $\approx 37,000$ years. (a)
 344 Temperature history. (b) Fluid pressure history. (c) Equilibrium gold solubility history. (d) Quartz solubility
 345 history. (e) Instantaneous quartz dissolution/deposition history. (f) Cumulative change history of quartz volume.

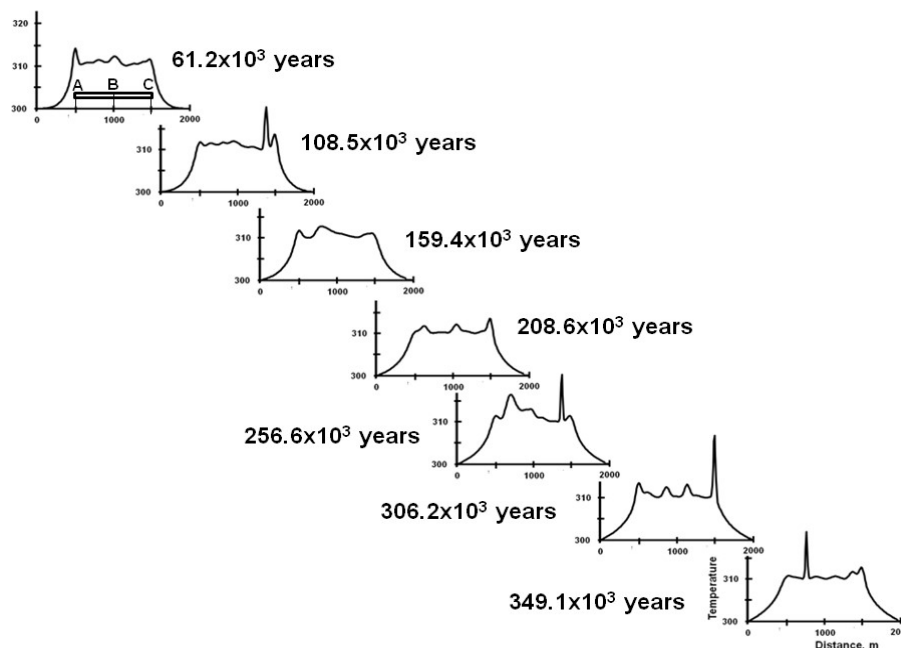
345

346 Figure 12.4 represents the behaviour of a medium temperature orogenic gold deposit
 347 where the extinction temperature is 310°C and the ignition temperature, 350°C . The heat
 348 absorbed by the reaction is 10^{-1} W m^{-3} and matches that produced by the deformation. Figure
 349 12.4 shows the histories, over a period of $\approx 37,000$ years, of temperature, fluid pressure,
 350 equilibrium gold solubility and quartz dissolution/precipitation history at the point
 351 corresponding to A in Figure 12.3. At this point in the system the temperature oscillations have
 352 a period of ≈ 620 years. The temperature behaviour overall as shown in Figure 12.5 and at any
 353 instant is spatially quite localised; the behaviour resembles that of a flickering flame. These
 354 spatial and temporal characteristics of the temperature behaviour arise from competition
 355 between heat generated by deformation at a site, the absorption of heat at that site by the
 356 endothermic reaction and the conduction of heat away or to that site from adjacent sites; the
 357 conduction process is sensitive to the thermal conductivity of the country rock.

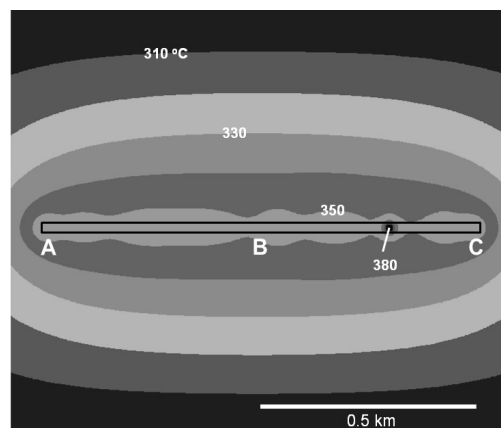
357

358 The fluid pressure, equilibrium gold solubility and quartz dissolution/precipitation
 359 histories mimic the temperature history since they depend only on the temperature although the
 360 fluid pressure and gold solubility histories are slightly out of phase with the temperature
 361 history; the fluid pressure slowly rises as more fluid is released from the chemical reaction.
 362 The magnitude of the fluid pressure is a function of competition between thermal expansion of
 363 the fluid due to a temperature change and the rate at which fluid pressure can diffuse from the
 364 site; eventually this competition results in a steady fluid pressure. Such competitive effects
 365 involving diffusion lead to the chaotic spatio-temporal behaviour observed. Although the fluid
 366 pressure fluctuations are small they are still sufficient to result in episodic mechanical failure if
 the stress state is initially close to failure.

367 The equilibrium gold solubility in this example, although episodic, still remains small
 368 at ≤ 0.5 ppm by weight in the fluid, consistent with the values of temperature and fluid
 369 pressure. These values of gold solubility are more than 0.2 ppm by weight in the fluid
 370 proposed by Loucks and Mavrogenes (1999) as a possible maximum for gold solubility carried
 371 by an entrance fluid. Hence the fluid in this system is not always saturated with gold but each
 372 temperature-fluid pressure drop means that gold is deposited as a solid. If the rate constant for
 373 gold deposition is much greater than the rate constant for gold dissolution then solid gold will
 374 slowly accumulate. At the position in the system corresponding to Figure 12.4 the total gold
 375 accumulated is ≈ 0.4 ppm by weight of rock after 37,000 years. Thus the grades of gold remain
 376 low but are localised because of the competitive processes mentioned above. This system
 377 would be characterised as a weakly mineralised hydrothermal system.

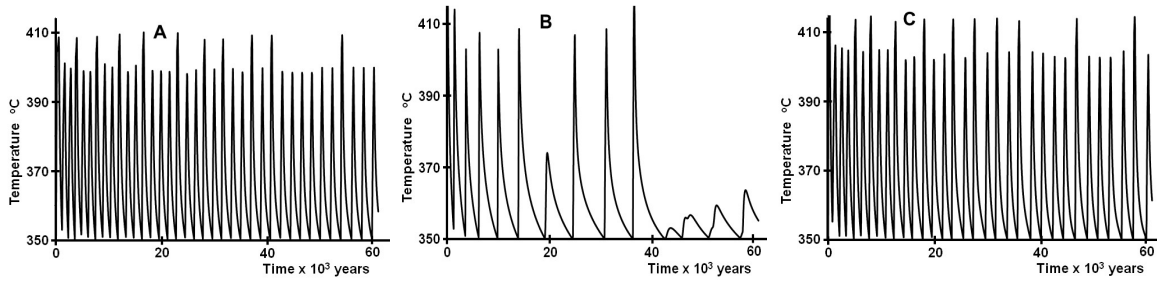


378
 379 Figure 12.5. Snapshots every 40 to 50,000 years of the temperature distribution in a longitudinal section across the
 380 centre of the hydrothermal system of Figure 12.4. The history resembles a flickering elongate combustion system.
 381
 382

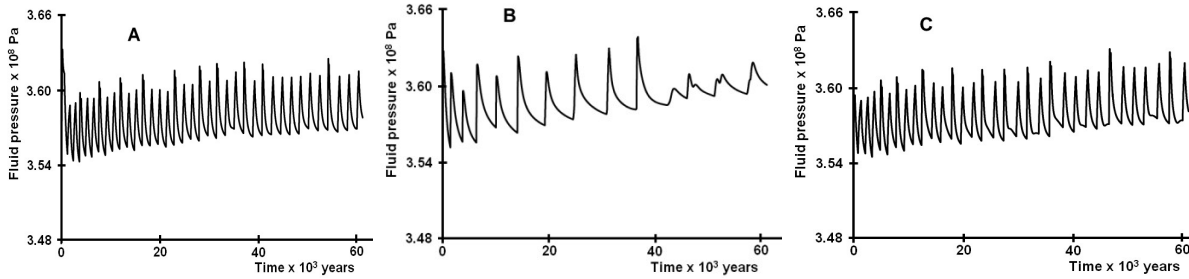


383
 384

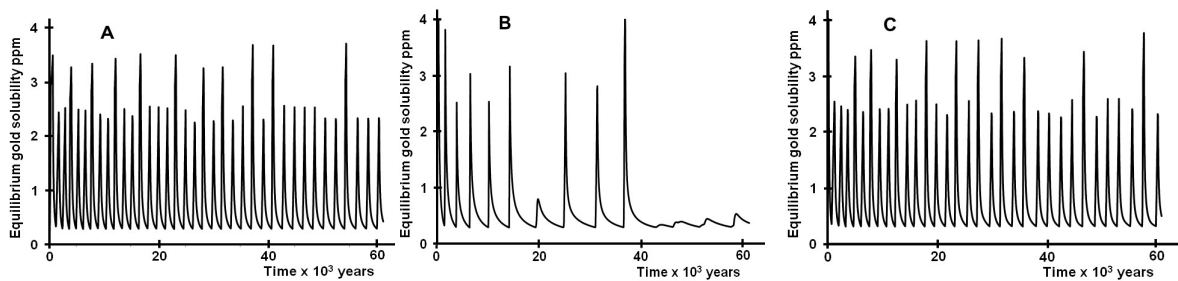
385



386



387



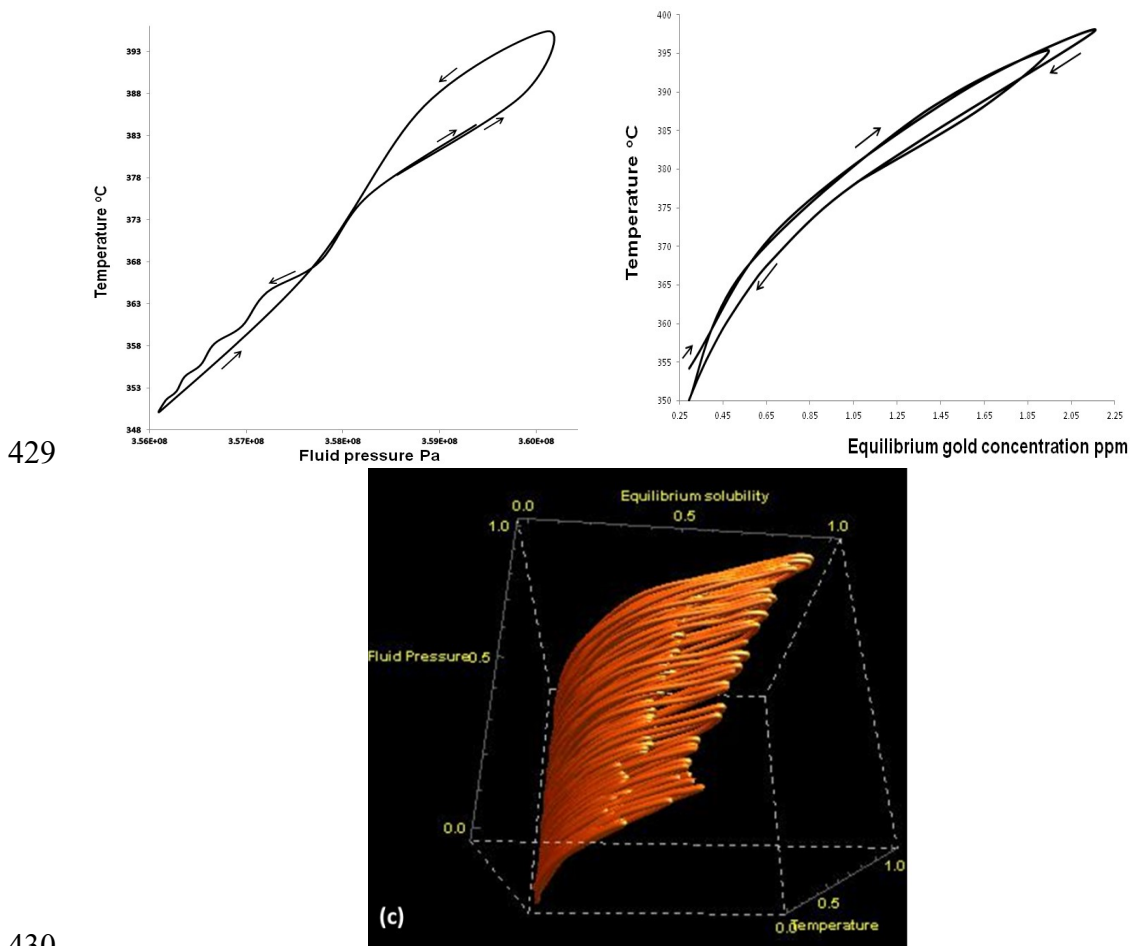
388 Figure 12.6. Episodic behaviour in a high temperature hydrothermal system with devolatilisation involving one
 389 exothermic reaction with kinetics given in Figure 8.11 (b). Fluids are released in the reaction and there is
 390 simultaneous continuous deformation. Top shows the temperature distribution at an instant. A, B, C are
 391 localities where histories are recorded in panels below. First row shows temperature histories at A, B, C. Middle
 392 row shows fluid pressure histories at A, B, C. Lower row shows equilibrium gold solubility histories at A, B, C.
 393

394 In Figure 12.6 we present a high temperature system where the extinction temperature
 395 is 350°C and the ignition temperature, 410°C. The heat absorbed by the reaction is 10^{-1} W m^{-3}
 396 and matches that produced by the deformation. Figure 12.6 shows the histories of temperature,
 397 fluid pressure and equilibrium gold solubility at three points in the hydrothermal system over a
 398 period of 60,000 years. In most parts of the system the oscillations have a period of $\approx 1,600$ to
 399 1,900 years whilst in the central regions the oscillations occur every $\approx 4,600$ years with a
 400 reduced maximum amplitude. The behaviour overall as shown at an instant in the top frame of
 401 Figure 12.6 is spatially quite localised. In the end regions the temperature sometimes does not
 402 reach the extinction temperature before falling again to the ignition temperature. These spatial
 403 and temporal characteristics of the temperature behaviour arise from competition between heat
 404 production from the exothermic reaction at a site and conduction of heat away or to that site
 405 from adjacent sites.

406 The fluid pressure and equilibrium gold solubility histories mimic the temperature
 407 history since they depend only on the temperature although the fluid pressure and gold
 408 solubility histories are out of phase with the temperature history since fluid is not released from
 409 the devolatilising reaction until after the peak temperature. The magnitude of the fluid pressure
 410 is a function of competition between thermal expansion of the fluid due to a temperature
 411 change and the rate at which fluid pressure can diffuse from the site. Such competitive effects
 412 involving diffusion lead to the chaotic spatio-temporal behaviour observed. Although the fluid

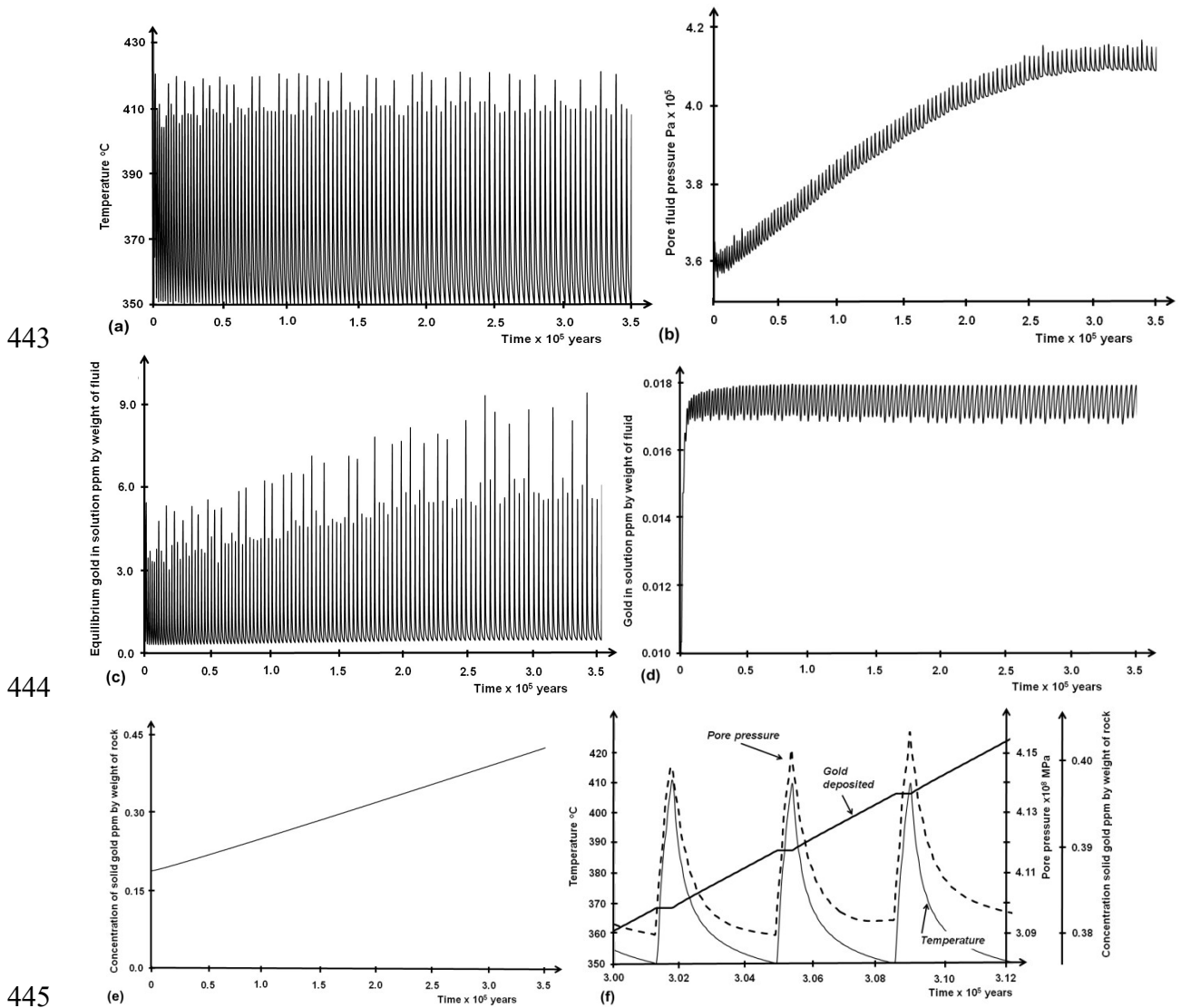
413 pressure fluctuations are small they are still sufficient to result in episodic mechanical failure if
 414 the stress state is initially close to failure.

415 The equilibrium gold solubility in this example, although episodic, reaches ≈ 3.5 ppm
 416 by weight in the fluid, consistent with the relatively high values of temperature and fluid
 417 pressure. These values of gold solubility are greater than 0.2 ppm by weight in the fluid
 418 proposed by Loucks and Mavrogenes (1999) as a possible maximum for gold solubility carried
 419 by an entrance fluid. Hence the fluid in this system is always under-saturated with gold and
 420 each temperature-fluid pressure drop means that gold is deposited as a solid only in amounts
 421 governed by the concentration of gold in solution. If the rate constant for gold deposition is
 422 much greater than the rate constant for gold dissolution then solid gold will slowly accumulate.
 423 At the ends of the system shown in Figure 12.6 the total gold accumulated is ≈ 7.5 ppm by
 424 weight of fluid in the rock or ≈ 0.3 ppm by weight of rock after 60,000 years or 2.5 ppm by
 425 weight of rock after 500,000 years. Thus the grades of gold can be significant but again are
 426 localised because of the competitive processes mentioned above. We discuss a quantitative
 427 model for gold deposition in the Discussion. The coupling between temperature, fluid pressure
 428 and equilibrium gold solubility is shown in Figure 12.7.



430
 431 Figure 12.7. Phase plots in temperature-fluid pressure – equilibrium gold solubility space. (a) A section in the
 432 temperature-fluid pressure plane. (b) A section in the temperature – equilibrium gold solubility plane. (c) The
 433 three dimensional phase plot with axes normalised to maximum values of temperature, equilibrium gold
 434 solubility and fluid pressure.
 435

436 In Figure 12.8 we show a relatively high temperature situation with a devolatilising
 437 endothermic reaction coupled to deformation. The parameters are the same as in Figure 12.6
 438 except that the permeability of the country rock is decreased to 10^{-20} m^2 and the thermal
 439 conductivity decreased to $2 \text{ W m}^{-1} \text{ K}^{-1}$. The result is an increased pore pressure since fluid
 440 pressure cannot leak easily from the system and an increase in the frequency of temperature
 441 oscillations since the system can heat up faster. The steady increase in pore pressure results in
 442 a steady increase in the equilibrium solubility of gold (Figure 12.8 c).



447 Figure 12.8. Episodic behaviour in a high temperature hydrothermal system with devolatilisation involving one
 448 exothermic reaction with kinetics given in Figure 8.11 (b). The net input of gold is $10^{-12} \text{ ppm s}^{-1} \text{ m}^{-2}$. Fluids are
 449 released in the reaction and there is simultaneous continuous deformation. The permeability of the country rock
 450 has been decreased, relative to Figure 12.6, to 10^{-20} m^2 and the thermal conductivity of the country rock is
 451 decreased to $2.0 \text{ W m}^{-1} \text{ K}^{-1}$ relative to Figure 12.6. Histories are at the equivalent position A in Figure 12.6. (a)
 452 History of temperature; oscillation period is ≈ 3000 years. (b) History of fluid pressure. (c) History of
 453 equilibrium gold solubility. (d) History of gold concentration in solution in ppm per weight of fluid as calculated
 454 from (12.9) and (12.10) in the Discussion. (e) History of deposited gold concentration in ppm per weight of rock
 455 as calculated from (12.11) and (12.12) in the Discussion. (f) Summary showing detail, over a period of 12,000
 456 years, of relations between temperature, fluid pressure and solid gold deposited; all oscillations are in phase.

458 12.4. Discussion.

459 12.4.1. Summary.

460 Here we summarise the results of this chapter before proceeding to a quantitative
461 model of gold deposition. In the early parts of the evolution of orogenic gold systems most
462 mineral reactions are exothermic and mineral reaction rates are dominated by the supply of
463 fluids to the reaction sites. The exothermic nature of the reactions together with the
464 exponential dependence of reaction rate on temperature and the linear dependence of reaction
465 rate on nutrient supply mean that reaction rates oscillate as the reaction rate competes with
466 the rate of supply of heat and of nutrients in incoming fluids. We have considered relatively
467 simple behaviour of the exothermic reaction, $A \rightarrow B$, but even more complex behaviour
468 occurs if nonlinear rates of heat supply/removal are taken into account (Chapter 8; Gray and
469 Scott, 1990, Chapter 7). The important point is that the reaction rate is highly sensitive to the
470 local fluid flow rate and so highly reacted parts of the rock mass can exist immediately
471 adjacent to unreacted parts simply because of differences in permeability and/or plastic-
472 chemical dilatancy.

473 The outcome of competition between fluid supply and temperature dependent reaction
474 rates is episodic fluctuations in temperature as the reaction cycles through ignition \rightarrow
475 extinction \rightarrow ignition phases as illustrated in examples in Chapter 8. These temperature
476 fluctuations produce fluctuations in fluid pressure which, in the absence of inelastic dilation,
477 have amplitudes governed by the rate at which fluid pressure can diffuse away from the
478 reaction site and on the thermal pressurisation coefficient, Λ , which lies in the range 0.1 to
479 0.9 MPa /C $^{\circ}$ and hence has an important effect. Such pressure fluctuations can initiate
480 fracturing and brecciation if the pore fluid is already close to being pressured lithostatically.

481 The important additional feature resulting from the fluctuations in pressure and
482 temperature is the episodic influence on the equilibrium solubility of gold and of other
483 important constituents of orogenic gold deposits, quartz and carbonates. Thus, assuming the
484 reaction $\text{AuHS}(\text{H}_2\text{S})_3^0 + 0.5\text{H}_2 \rightarrow \text{Au} + 4\text{H}_2\text{S}$ and the results depicted in Figure 12.2 the
485 system oscillates with respect to the equilibrium solubility of gold as shown in Figures 12.3,
486 12.4, 12.6 and 12.8. Many authors including Loucks and Mavrogenes (1999) and Henley and
487 Berger (2000) have pointed to the difficulty in reaching the high equilibrium solubilities
488 indicated in Figure 12.2 and modelled in Figures 12.3, 12.4, 12.6 and 12.8. Loucks and
489 Mavrogenes (1999) indicate that 0.2 ppm by weight of gold in solution is near a maximum
490 one could expect to see in any inlet feed supply to a gold system. In this chapter we mainly
491 assume an input gold concentration of 10 ppb by weight of fluid. Hence there is a problem in
492 developing the high bonanza grades (ounces per tonne of rock) that are seen in some gold
493 deposits.

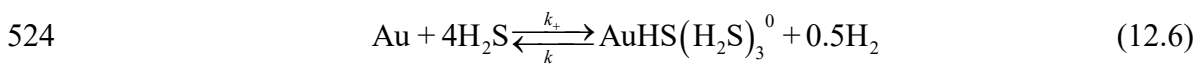
494 For the low temperature situation shown in Figure 12.3 we see about 13 oscillations in
495 temperature and fluid pressure in a period of 60,000 years. The results for the equilibrium
496 solubility of gold in this system show that the fluids in the system are saturated with gold for
497 all of the history of alteration so that gold is deposited every time the pressure and
498 temperature drop. In such a system gold concentrations of $\approx 10^{-2}$ ppm by weight of rock is an
499 upper limit to the grades that could develop if the system lasts 500,000 years. Thus the
500 deposit although strongly altered is very weakly mineralised.

501 For the medium temperature situation shown in Figure 12.4 there are about 60
 502 oscillations in temperature and fluid pressure in a period of $\approx 36,000$ years. The concentration
 503 of gold in solution exceeds that we could expect as the equilibrium solubility in any incoming
 504 stream so the system is under-saturated with respect to gold until the equilibrium solubility
 505 reaches low values. We expect a deposit of disseminated, interesting grades of gold, reaching
 506 perhaps 1-2 grams per tonne.

507 For the higher temperature situation shown in Figure 12.6 we see about 37 oscillations
 508 in temperature and pressure over 60,000 years with equilibrium concentrations of gold
 509 oscillating between ≈ 0.2 and ≈ 4 ppm by weight in the fluid. The issue now in this high
 510 temperature situation is whether the concentration of gold in solution can rise above say 0.2
 511 ppm by weight or is it fixed at the inlet concentration of $\ll 0.2$ ppm throughout each cycle?
 512 If the fluid remains under-saturated throughout its history with a concentration of 0.2 ppm by
 513 weight of fluid then the grade of the deposit at end locations will be ≈ 0.3 ppm by weight of
 514 rock if the system lasts for 60,000 years or ≈ 3.3 ppm by weight of rock if the system lasts for
 515 10^6 years. These relatively low grades suggest that gold enhancement process may operate in
 516 some systems to increase the gold concentration in solution towards equilibrium values as the
 517 system evolves. Below we present a model that enables such enhancement as the system
 518 evolves through a process that involves deposition of gold as the temperature and pressure
 519 drops in a particular cycle and relatively minor dissolution of deposited gold as the
 520 temperature and pressure rise in the next cycle. We then consider localisation behaviours that
 521 can lead to bonanza grades of gold.

522 **12.4.2. A model for progressive enrichment of gold in solution.**

523 We consider the reaction



525 where k_+ and k_- are the rate constants for the dissolution and deposition reactions
 526 respectively. Since the reaction proceeding to the right is endothermic we expect from
 527 transition state theory, that the temperature dependence of the rate constant for deposition of
 528 gold, $k_{deposition}$, is greater than that for the rate constant for dissolution, $k_{dissolution}$ (Schott et al.,
 529 2009). Both the dissolution and deposition processes are heterogeneous and so both the rates
 530 of deposition and of dissolution of gold depend on the concentration of gold in solution and
 531 the amount of gold precipitated. By analogy with processes that operate in fixed bed chemical
 532 reactors (Aris, 1975) the precise mechanisms of gold deposition and dissolution and their
 533 dependencies on solid gold concentration are likely to be quite complicated but we assume
 534 simple linear dependencies for the want of better models. In the limited modelling we have so
 535 far considered the precise mechanism makes little difference to the qualitative behaviour of
 536 the system. In addition, gold is added to the system in solution at a constant rate. In what
 537 follows we consider gold dissolution and deposition processes as the temperature and pore
 538 pressure rise and fall as in the histories depicted in Figures 12.6 and 12.8.

539 ***Change in gold concentration during a temperature/fluid pressure increase.***

540 We assume a system in which the reaction (12.6) occurs. The problem we want to
 541 consider involves episodic changes in temperature and fluid pressure so that the equilibrium
 542 solubility of gold fluctuates in time as do the rate constants, through an Arrhenius

543 dependence, as the temperature changes. These changes also produce episodic fluctuations in
 544 the activities of H₂ and of H₂S. Since the forward and reverse reactions are heterogeneous the
 545 rates of the reactions also depend on the current surface area of solid gold. The problem of
 546 tracking the deposition of gold is therefore quite complex with different behaviours
 547 depending on the evolving variables, temperature, pore pressure, equilibrium gold solubility,
 548 the activities of gaseous phases and the gold surface area. Instead of exploring the complete
 549 parameter space involving these variables, we explore a subsection of parameter space and
 550 adopt a simple approach to the problem in which the fluctuations in rate constants,
 551 equilibrium gold solubility and surface area can be explored.

552 We begin by writing the rates of gold dissolution and deposition in the following
 553 ways:

$$554 \quad \frac{dx}{dt} = \delta + k'_+ x \left(1 - \frac{x}{x^*}\right) y \quad (12.7)$$

$$555 \quad \left[\begin{array}{c} \text{Rate of change} \\ \text{of gold in} \\ \text{solution} \end{array} \right] = \left[\begin{array}{c} \text{Net rate of} \\ \text{addition of} \\ \text{gold in} \\ \text{solution} \end{array} \right] + \left[\begin{array}{c} \text{Rate of dissolution of} \\ \text{gold modified by a} \\ \text{saturation term} \end{array} \right]$$

$$556 \quad \frac{dy}{dt} = -k'_- xy \quad (12.8)$$

$$557 \quad \left[\begin{array}{c} \text{Rate of change} \\ \text{of solid gold} \end{array} \right] = - \left[\begin{array}{c} \text{Rate of solution of} \\ \text{gold} \end{array} \right]$$

558 In these equations x and y are the concentrations of gold in solution and of solid gold, t is
 559 time, k'_+ , k'_- are the forward and reverse rate constants expressed as functions of the activities
 560 of H₂S and of H₂, that is, $k'_+ = k_+ a_{\text{H}_2\text{S}}^4$ and $k'_- = k_- a_{\text{H}_2}^{1/2}$. Both these rate constants follow an
 561 Arrhenius relation: $k = k^0 \exp(-E_a / RT)$. x^* is the current equilibrium solubility of gold, δ is
 562 the net flux of gold in solution into the system and the term $\left(1 - \frac{x}{x^*}\right)$ expresses the slowing of
 563 the dissolution rate as the equilibrium solubility is approached so that the dissolution rate is
 564 zero when $x = x^*$. The dissolution rate of gold also slows as $y \rightarrow 0$. (12.7) is a form of
 565 logistic equation which has been well explored; Banks (1994) discusses the behaviour of this
 566 equation for situations where δ , the k 's and x^* are functions of time.

567 In all the following models we assume the following values for parameters:
 568 $k_{+}^{0'} = 1.97 \times 10^{-3} \text{ mol s}^{-1}$, $k_{-}^{0'} = 1.97 \times 10^{-1} \text{ mol s}^{-1}$, $E_{a+} = 1.1 \times 10^5 \text{ J mol}^{-1}$; $E_{a-} = 1.0 \times 10^4 \text{ J mol}^{-1}$.
 569 We have explored wide variations in these parameters and the behaviour of the system seems
 570 insensitive to the values selected.

571 Although it is unlikely that the concentration of gold in solution ever reaches the
 572 higher values of equilibrium gold solubility, x^* , shown in Figures 12.6 and 12.8, x^* is still an
 573 important parameter since it has an instantaneous influence on the rate of dissolution through
 574 (12.7). At low values of x^* , dissolution is inhibited or prevented, whereas at high values of x^* ,
 575 dissolution is enhanced.

576 ***Change in gold concentration during a temperature/fluid pressure decrease.***

577 For that part of a cycle where there is a decrease in temperature and fluid pressure we
 578 write for the rates of change of gold in solution and for gold deposited logistic equations of
 579 the forms (12.9) and (12.10).

$$\frac{dx}{dt} = \delta - k'_x \left(1 - \frac{x}{x^*}\right)$$

580
$$\begin{bmatrix} \text{Rate of change} \\ \text{of gold in} \\ \text{solution} \end{bmatrix} = \begin{bmatrix} \text{Net rate of} \\ \text{addition of} \\ \text{gold in} \\ \text{solution} \end{bmatrix} - \begin{bmatrix} \text{Rate of} \\ \text{deposition of} \\ \text{solid gold} \end{bmatrix} \quad (12.9)$$

$$\frac{dy}{dt} = k'_x \left(1 - \frac{x}{x^*}\right)$$

581
$$\begin{bmatrix} \text{Rate of change} \\ \text{of gold being deposited} \end{bmatrix} = \begin{bmatrix} \text{Rate of} \\ \text{deposition of} \\ \text{gold as solid} \end{bmatrix} - \begin{bmatrix} \text{Rate of} \\ \text{solution of} \\ \text{solid gold} \end{bmatrix}$$

582
$$(12.10)$$

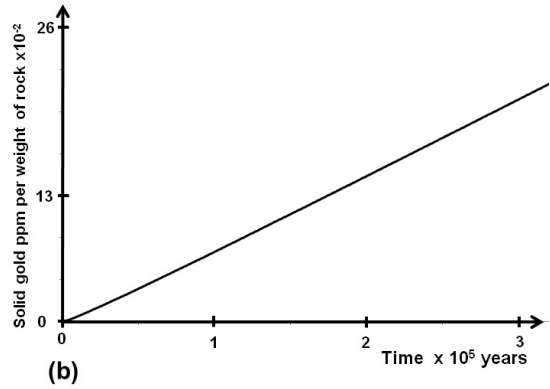
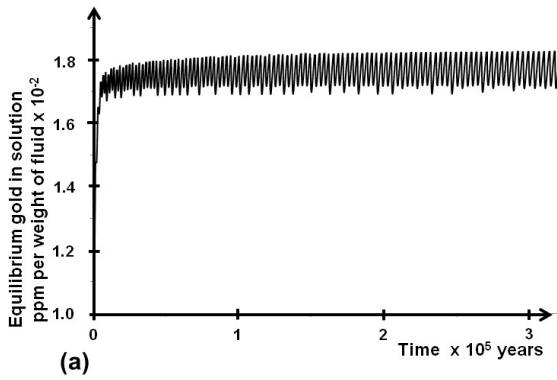
583 For the temperature-fluid pressure decrease part of the cycle we first explore the equations as
 584 written in (12.9) and (12.10) and then explore a situation where the deposition rates depend
 585 on the concentration of solid gold as in (12.11) and (12.12).

586
$$\frac{dx}{dt} = \delta - k'_x(1-y)y \quad (12.11)$$

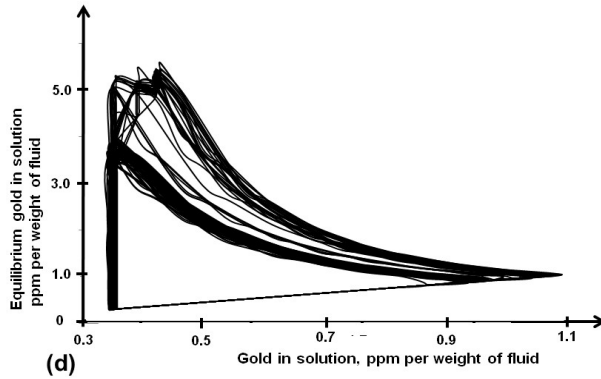
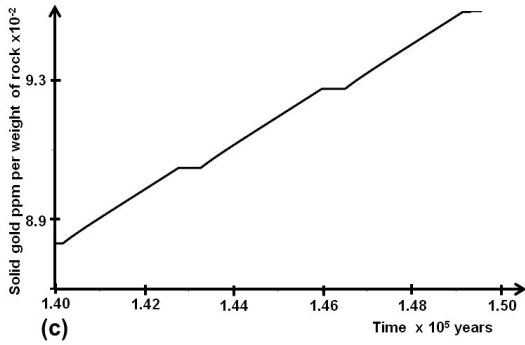
587
$$\frac{dy}{dt} = k'_x(1-y)y \quad (12.12)$$

588 The behaviour of gold dissolution and deposition is shown for three situations in
 589 Figures 12.9, 12.10 and 12.11 for the high temperature model of Figure 12.6. Figure 12.9
 590 shows the effect of decreasing the thermal conductivity and permeability of the country rocks
 591 starting from an initial solid gold concentration of 0.185 ppm by weight of rock. The
 592 efficiency of the gold deposition process is 68% which represents an increase of 57% over
 593 situations where the thermal conductivity of the country rocks is $2.25 \text{ W m}^{-1} \text{ K}^{-1}$. Figures
 594 12.10 and 12.11 highlight the differences in grade resulting from net input flows of 10^{-12} and
 595 $10^{-10} \text{ ppm m}^{-2} \text{ s}^{-1}$. The wall rock thermal conductivity is $2.25 \text{ W m}^{-1} \text{ K}^{-1}$.

596



597



598

599

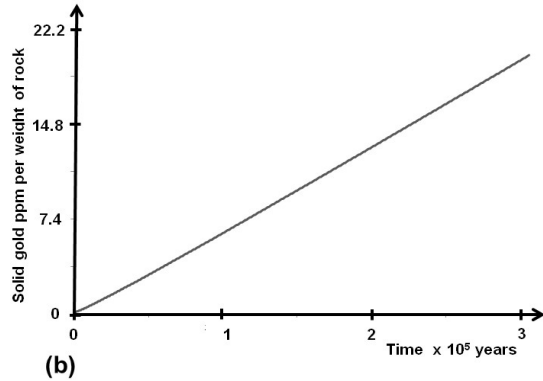
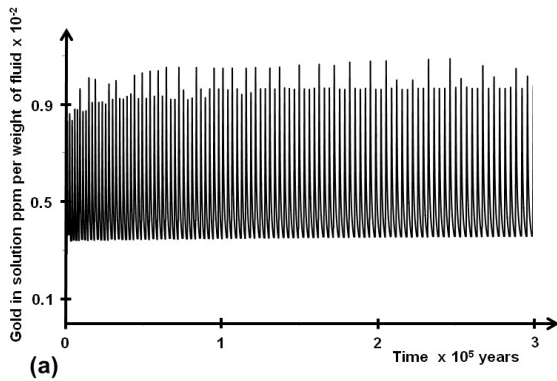
600

601

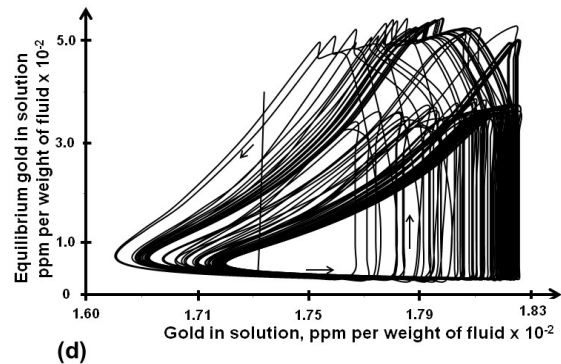
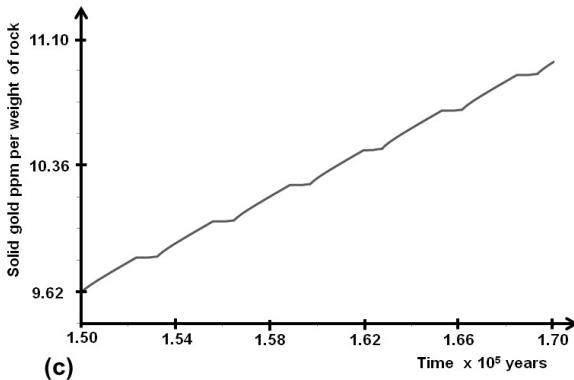
602

Figure 12.9. Solutions to (12.7) and (12.8) for $\delta = 10^{-12}$ ppm $m^{-2} s^{-1}$, $x_0 = 10^{-2}$ ppm and $y_0 = 10^{-2}$ ppm. Other parameters are given in the text. Model is the same as Figure 12.6. (a) Concentration of gold in solution in ppm by weight of fluid. (b) Concentration of solid gold in ppm per weight of rock. (c) Detail of (b) showing periods of deposition oscillating with periods of negligible dissolution or deposition. (d) The attractor in phase space: equilibrium solubility of gold – concentration of gold in solution.

603

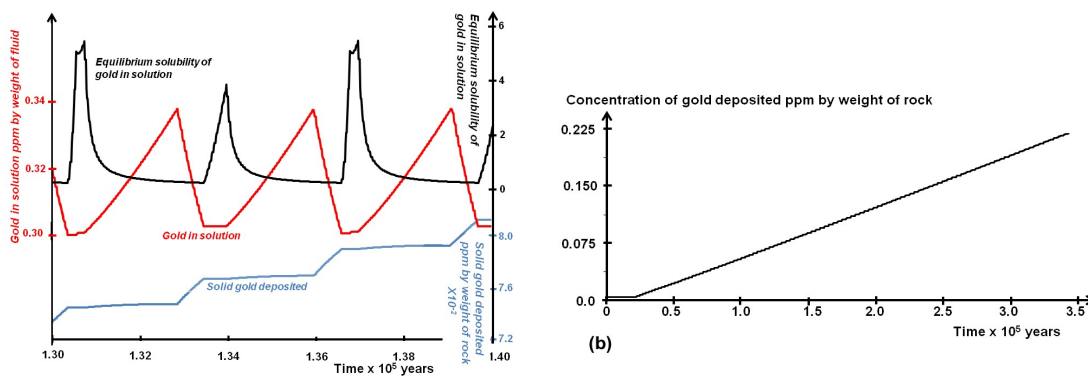


604



605 Figure 12.10. Solutions to (12.9) and (12.10) for $\delta = 10^{-10}$ ppm m⁻² s⁻¹, $x_0 = 10^{-2}$ ppm and $y_0 = 10^{-2}$ ppm. Other
 606 parameters are given in the text. Model is the same as Figure 12.6. (a) Concentration of gold in solution in ppm
 607 by weight of fluid. (b) Concentration of solid gold in ppm per weight of rock. (c) Detail of (b) showing periods
 608 of deposition oscillating with periods of negligible dissolution or deposition. (d) The attractor in phase space:
 609 (equilibrium solubility of gold – concentration of gold in solution).

610 In Figure 12.11 we show some of the results for a more complicated gold deposition
 611 process given by (12.11) and (12.12). The gold dissolution process is now out of phase with
 612 respect to the equilibrium concentration of gold in solution (Figure 12.11 a) but this makes
 613 little difference to the overall gold grade (Figure 12.11 b). Since the equilibrium gold
 614 concentration in solution is in phase (not shown) with the pore pressure this means that gold
 615 deposition is not coincident with brecciation or fracturing events that occur as the effective
 616 stress reaches the yield stress.



617 Figure 12.11. Solutions, over a time period of 10,000 years, to (12.11) and (12.12) for $\delta = 10^{-12}$ ppm m⁻² s⁻¹,
 618 $x_0 = 10^{-2}$ ppm and $y_0 = 10^{-2}$ ppm. Other parameters are given in the text. Otherwise the model is the same as
 619 Figure 12.6. (a) Summary of coupling between equilibrium gold in solution, gold in solution and solid gold
 620 deposited. (b) History of solid gold deposited in ppm by weight of rock over 350,000 years.

622 12.5. Parameter space.

623 In this chapter we have explored a very restricted part of the parameter space that
 624 describes the various behaviours of a highly nonlinear system. The aim has been to select a
 625 simple subset of the system in which the basic principles of nonlinear behaviour can be
 626 demonstrated. As we indicated earlier some of the dimensionless parameters that describe
 627 behaviour in this subset are:

- 628 • The Damköhler number, Da , is a measure of the importance of the time scale of fluid
 629 flow relative to that for chemical reaction. In the system we examined changes in Da
 630 result in simple oscillatory behaviour of the chemical reaction. In many systems (Gray
 631 and Scott, 1990) the control of Da on the chemical reaction rate is much more
 632 complicated.
- 633 • The Newtonian cooling time measures the importance of the thermal cooling time scale
 634 relative to the chemical time scale. This is also important in controlling chemical reaction
 635 rates (Aris, 1999). It is influenced strongly by the shape of the system and by the thermal
 636 conductivity of the wall rocks and so is important in studies of specific orogenic gold
 637 systems; we expect systems of different shapes to behave in different manners as
 638 discussed below. The limited exploration we have done indicates that systems with a wall

639 rock thermal conductivity of $1.8 \text{ W m}^{-1} \text{ K}^{-1}$ have gold grades 17% higher than if the wall
640 rock thermal conductivity is $4 \text{ W m}^{-1} \text{ K}^{-1}$.

641 • The Arrhenius number, Ar , measures the importance of the thermal energy relative to the
642 activation energy for chemical reactions and for rate sensitive deformation processes. Ar
643 defines the spectrum of chemical reactions that occur in a particular system (Law, 2006,
644 pp 60-62) and hence is fundamental in defining the paragenetic sequence we see in a
645 particular system. Ar is also fundamental in defining the deformation behaviour of the
646 system (Veveakis et al., 2010).

647 In addition, two other dimensionless numbers need to be included in any extension of
648 what has been done here:

649 • The Gruntfest number, Gr , measures the importance of the heat generated by deformation
650 to that absorbed or generated by chemical reactions. Gr is important in defining the
651 magnitude of the temperature increase possible for coupled deformation/chemical
652 reactions and hence influences the deformation rate in systems where rate dependent
653 constitutive behaviour is included (Veveakis et al., 2010, 2014; Alevizos et al., 2014;
654 Poulet et al., 2014).

655 • The Lewis number, Le , is a measure of the importance of heat transport by diffusion to
656 mass transport. Le is important in defining the magnitude of the pore pressure increase
657 possible for a particular temperature increase as fluid diffuses from the site of the
658 temperature increase (Veveakis et al., 2014; Alevizos et al., 2014; Poulet et al., 2014). In
659 the systems explored here the wall rocks for the system are relatively permeable and
660 hence pore pressure leaks away as devolatilisation proceeds and the temperature
661 increases. If the wall rocks are relatively impermeable, as would be the case for instance
662 if the system is embedded in black shales, the Lewis number is smaller and the pore
663 pressure increases would be larger.

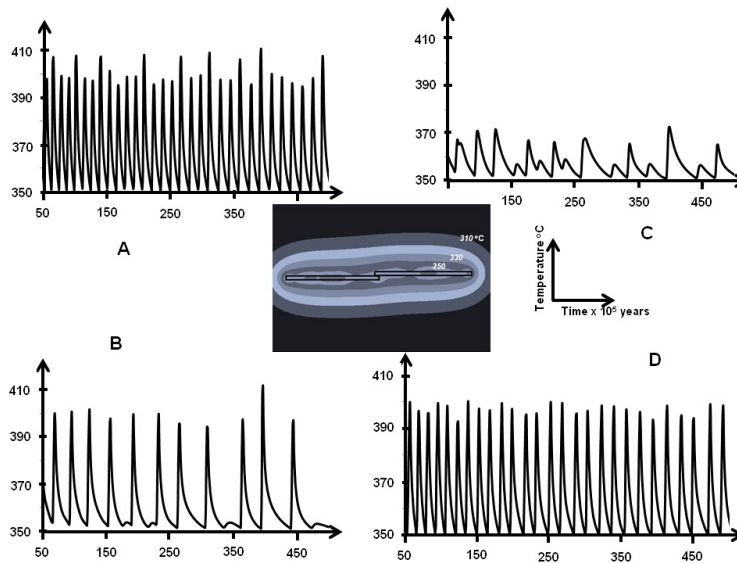
664 Future work needs to concentrate on exploration of what are envisaged to be important
665 parts of this five-fold parameter space. For some systems parts of this space will be more
666 relevant than others.

667

668 **12.6. The influence of geometry.**

669 Since the chemical reaction rates in an open flow thermodynamic system are highly
670 sensitive to the supply of heat to the system and the oscillatory behaviour is sensitive to the
671 rate at which heat can be lost from the system, the cooling regime becomes an important
672 parameter in controlling the behaviour of the system. An important element in this control is
673 the ratio of the surface area of the reacting system to its volume. To illustrate this effect in
674 Figure 12.12 we show the behaviour of a system very similar to that modelled in Figures
675 12.3, 12.4, 12.6 and 12.8 but with an offset, and hence a thickening, of the system in the
676 central region. This change in geometry results in changes in the heat diffusing from the
677 central region to the country rock and in heat diffusing from adjacent areas of the reacting
678 system. The thermal behaviour in this central region is now quite different to that in Figures
679 12.3, 12.4, 12.6 and 12.8 with more oscillations in temperature and larger amplitudes of

680 fluctuations in the thickened region. Thus we expect the system shown in Figure 12.12 to
 681 produce higher grades of gold than in the thinner geometries.



682

683 Figure 12.12. Episodic behaviour in a system involving one exothermic reaction with kinetics given in Figure
 684 8.11 (b). No fluids are released in the reaction and there is no deformation. Middle panel shows the temperature
 685 distribution at an instant. A, B, C, D are localities where histories are recorded in panels below. Remaining
 686 panels shows temperature histories at A, B, C and D.

687 12.7. What controls the grade of an orogenic gold deposit?

688 The maximum gold grade, $g^{maximum}$, possible in a deposit is the integrated flux of gold
 689 into the system over the lifetime, $t^{lifetime}$, of the deposit:

690

$$g^{maximum} = \int_0^{t^{lifetime}} \delta dt$$

691 In the absence of any processes that localise gold deposition this grade will be uniformly
 692 distributed in the system. With $\delta = 2.7 \times 10^{-12}$ ppm by weight of fluid $m^{-2} s^{-1}$ over 500,000
 693 years, $g^{maximum} = 1.58$ ppm by weight of rock. This corresponds to a fluid flux through a
 694 system with a lithostatic pore pressure gradient, a permeability of $10^{-17} m^2$, a fluid viscosity
 695 of $10^{-4} Pa s$, an input gold concentration in solution of 1 ppb by weight of fluid and perhaps
 696 losses in the outflow of 0.1 ppb by weight of fluid. Any change in these values will change
 697 the result proportionally but these values seem reasonable and conservative. If for instance
 698 the permeability was increased to $10^{-16} m^2$ then the maximum grade is 15.8 ppm by weight of
 699 rock. Thus it seems possible but difficult to reach bonanza grades of many ounces per tonne
 700 (1 ounce troy $tonne^{-1} = 31.1 g tonne^{-1}$). Even a grade of 1ppm per weight of rock requires a
 701 mechanism to deposit the gold from solution and we are proposing that aseismic intrinsic
 702 oscillations in temperature as described here are one way of achieving this. High bonanza
 703 grades require some process for localisation of gold deposition within the system and we
 704 discuss such processes later in the Discussion. In the models presented here the system
 705 always loses gold in solution as the mineralising process proceeds. In general the efficiency,
 706 measured by the ratio of amount of gold deposited in the system to the amount of gold added
 707 to the system, is $\approx 57\%$. In Figure 11 (e) where the thermal conductivity of the country rock
 708 has been reduced to $2 W m^{-1} K^{-1}$ the efficiency rises to $\approx 68 \%$.

709 The critical factors required to optimise gold grades in a system with episodic
710 behaviour are processes that maximise the temperature and pore fluid pressure so that the
711 equilibrium solubility of gold is maximised (see Figure 12.2). The temperature is controlled
712 by the ΔH of mineral reactions that occur at the time of gold deposition together with heat
713 liberated by deformation. Strongly exothermic reactions and fast deformation rates lead to
714 higher frequency temperature oscillations than for situations with endothermic reactions and
715 no deformation. Temperatures are higher if the country rocks have low thermal conductivity
716 typical of shales or pelites in general. Fluid pressure depends on three factors: The
717 temperature, concurrent release of fluids from devolatilising reactions and the permeability of
718 the country rocks; low permeability rocks such as pelites, quartzites and mafic rocks inhibit
719 the leakage of fluid pressure from the system and hence result in higher fluid pressures. All of
720 these factors are recorded in the paragenetic sequence and in the relation of this sequence to
721 the deformation history. The key to understanding orogenic gold systems is to view them in
722 terms of the energy balance between chemical, hydrological, thermal and deformation
723 processes that are observed in the system.

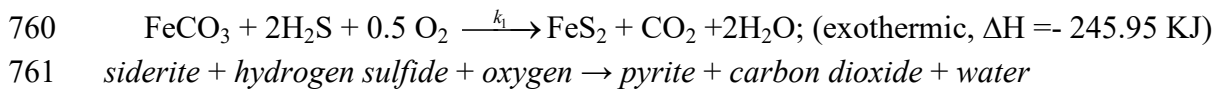
724 The early stage of alteration in a system where exothermic reactions dominate and
725 fluids such as CO_2 and H_2O are consumed to produce carbonates and hydrous silicates, in a
726 sense, serves to set the system up for a later mineralisation stage. This early stage increases
727 the temperature of the system so that reactions with larger activation energies can ignite and
728 provides a readily available source of stored CO_2 and H_2O in mineral crystal structures for
729 access at a later stage. The low temperatures and the consumption of fluids, both of which
730 contribute to low fluid pressures, mean that the equilibrium solubility of gold is small and
731 mineralisation, if present, is of low grade.

732 The later stages of system evolution involve higher temperatures and the release of
733 fluids. Hence higher fluid pressures develop if the permeability structure of the system allows
734 this to happen. Such an environment may, for example, consist of an envelope of black
735 shales, or fractures in an impermeable quartzite, mafic rock or older quartz vein. The high
736 fluid pressures generated by high temperatures, devolatilisation and a low permeability
737 envelope are essential for the development of high equilibrium solubilities of gold. It is
738 perhaps important that many large gold deposits are hosted in shale or pelite environments
739 (Wood and Popov, 2006; Wilson et al., 2009, 2013).

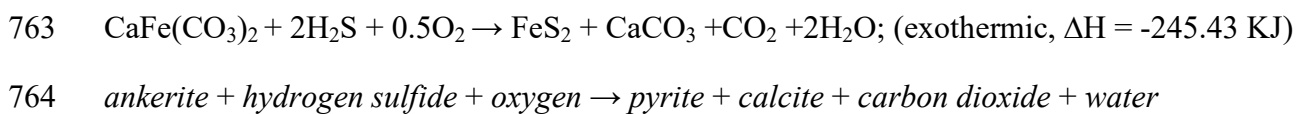
740 Orogenic gold systems resemble open flow packed bed chemical reactors (Aris, 1975;
741 Rawlings and Ekerdt, 2013, Chapter 7) in that there is a strong coupling between fluid flow,
742 thermal transport and chemical reactions. As such they are described by some form of
743 reaction-advection-diffusion equation as presented in (1). An important difference between
744 an orogenic gold system and a conventional fixed bed reactor of the chemical engineer is that
745 deformation is an important dissipative process that is absent in fixed bed chemical reactors.
746 Reaction-advection-diffusion equations generally lead to spatio-temporal patterning and the
747 results presented in this chapter are some examples of such patterning.

748 There is a special form of spatio-temporal behaviour that occurs in reaction-advection
749 systems where exothermic and endothermic reactions are coupled. These patterns, called
750 travelling waves, consist of strong localisations of temperature that move through the system
751 at speeds (the group velocity) that are generally less than the speed associated with a material
752 particle. In some cases the travelling wave localises into a soliton. Examples are given by

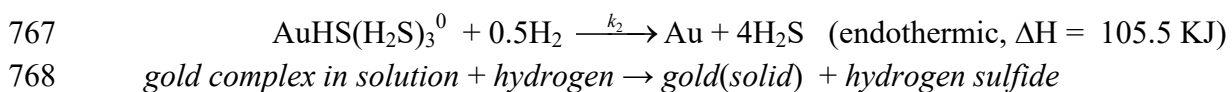
753 Ball et al. (1999), Hmaidi et al. (2010), Sharples et al. (2012) and Forbes (1997, 2013a, b).
 754 These thermal solitons differ from classical standing waves in water (Whitham, 1974) in that
 755 they “sweep-up” any smaller thermal anomalies as they move so that the temperature in the
 756 largest soliton increases as the system evolves (Forbes, 2013 a). We propose that this kind of
 757 thermal soliton is responsible for producing bonanza grades (ounces per ton) of gold in some
 758 deposits. A typical reaction-advection system that might be capable of thermal soliton
 759 behaviour is shown in Figure 12.13 (a) where either of the reactions



762 or,



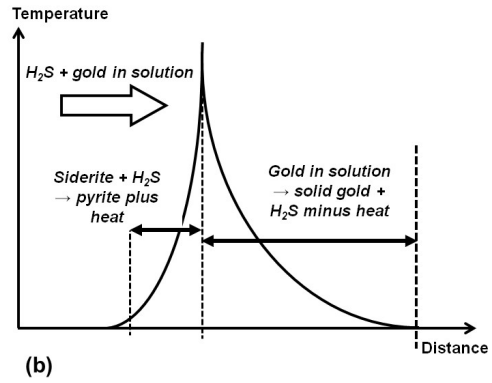
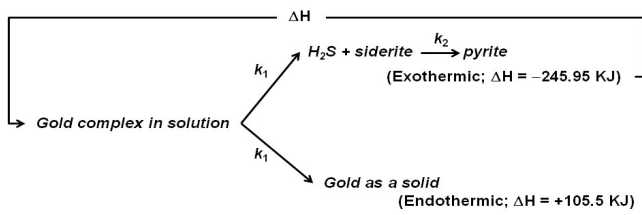
765 proceed at the same time as the deposition of gold from solution during temperature and fluid
 766 pressure drops expressed by



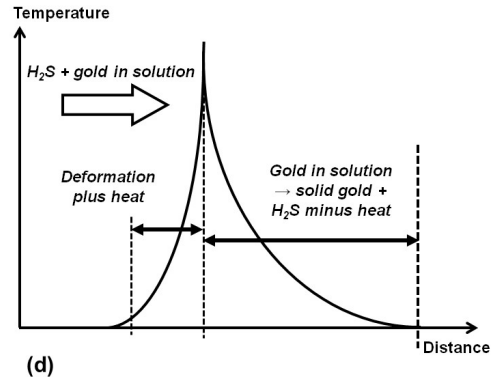
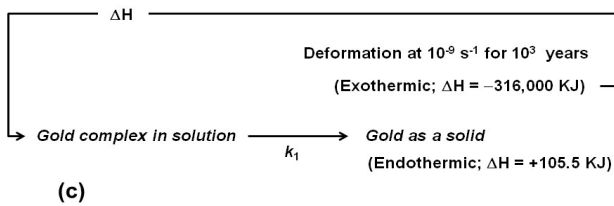
769

770 Here the H₂S produced by the deposition of gold (an endothermic process) is used to react
 771 with siderite to produce pyrite (an exothermic process). The pyrite forming process releases ≈
 772 246 KJ of heat which is used to amplify the gold deposition process which requires ≈ 106 KJ
 773 of heat. The remaining 140 KJ of heat can be used to increase the temperature and hence
 774 increase both the siderite to pyrite and gold deposition rates. This kind of coupled reaction
 775 system when coupled with advective transport leads to a thermal soliton where the pyrite
 776 production process proceeds in the tail of the soliton and drives the gold deposition process in
 777 the soliton front (Figure 12.13 b). This kind of process needs to be integrated into the
 778 episodic behaviour reported in the main body of this chapter.

779 A similar process involves the heat released by localised deformation (Figures 12.13
 780 c, d) as gold in solution is advected into the high temperature spike associated with the
 781 deformation. The increased heat in the upstream tail of the spike is used to drive the
 782 endothermic gold deposition process in the downstream front of the spike. An example where
 783 such localisation processes may have operated is given by Fougrouse et al. (2016) for the
 784 Obuasi gold deposit. Here there is widespread evidence of remobilisation of gold associated
 785 with localised deformation at the scale of 1 km and at the cm-scale associated with
 786 crenulation cleavages. Early high grades of gold (5 to 6 g/ton) are associated with the
 787 exothermic reaction: H₂S + ankerite → arsenopyrite and synchronous pervasive deformation,
 788 whereas grades of 15 g/ton are associated with later localised deformation (Fougrouse et al.
 789 2015; 2016 a, b).



790



791

792 Figure 12.13. The development of thermal solitons. (a) Thermal feedback between gold deposition reaction and
 793 pyrite formation reactions. (b) Formation of a thermal soliton with spatial distributions of the siderite to pyrite
 794 reaction (exothermic) and the gold deposition reaction (endothermic). The direction of fluid flow is shown
 795 advecting H_2S and gold in solution. (c) Thermal feedback between gold deposition reaction and deformation. (d)
 796 Formation of a thermal soliton with spatial distributions of deformation (exothermic) and the gold deposition
 797 reaction (endothermic). The direction of fluid flow is shown advecting H_2S and gold in solution.

798 12.8. The implications of chaos.

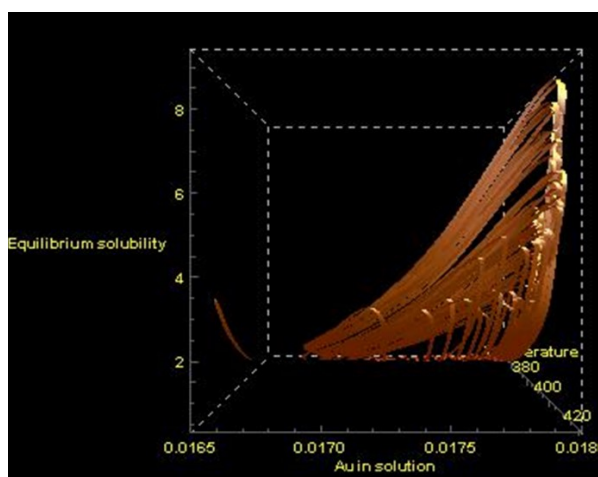
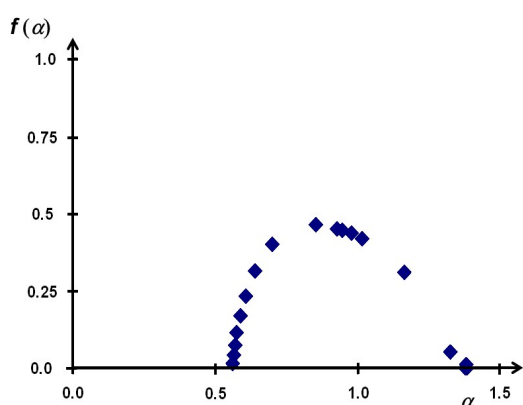
799 The system we have described here behaves in an episodic but apparently stochastic
 800 manner in that the future of the system from any instant can only be predicted using
 801 probabilities. In addition, slight changes in operating conditions such as spatial position,
 802 permeability and thermal conductivity result in different behaviours. The stochastic
 803 behaviour and sensitivity to changes in operating conditions means that the system behaviour
 804 can be regarded as chaotic (Sprott, 2003). Even so the behaviour is the result of clearly
 805 defined physical and chemical rules so that the chaos is deterministic.

806 Systems that exhibit deterministic chaos commonly have two characteristic features.
 807 First, the large (in principle, infinite) number of states that the system occupies means that the
 808 system should be multifractal (Beck and Schlögl, 1993). These states are defined by
 809 temperature, fluid pressure, equilibrium gold solubility, gold in solution and deposited gold.
 810 Thus although the system evolves through a large number of states, some states occur more
 811 often than others. The frequencies of states are referred to as *singularities* and the intensity of
 812 the frequency is the *singularity strength*, commonly labelled, α (Feder, 1988). The chaotic
 813 nature of the system means (Beck and Schlögl, 1993) that the singularities occur in a manner
 814 such that each singularity strength is distributed in a fractal manner with its own fractal
 815 dimension, $f(\alpha)$. Thus the system can be thought of as a population of different singularities
 816 embedded in each other each with a different fractal dimension. Such a population is a

817 multifractal and can be represented as a singularity spectrum which is, from a statistical
818 mechanics point of view, the entropy function for the system (Beck and Schlögl, 1993;
819 Arneodo et al., 1995). In Figure 12.14 (a) we show the singularity spectrum for the
820 temperature history shown in Figure 12.6 (a). The spectrum is well defined as is to be
821 expected from a system exhibiting deterministic chaos.

822 The multifractal nature of the systems modelled in this chapter means that although
823 the behaviour is chaotic, the system can be characterised by its singularity spectrum. Such
824 spectra have different characteristics according to the physical and chemical processes that
825 produced the system and can be symmetrical or asymmetrical, narrow or broad and have
826 large or small values of the maximum value of $f(\alpha)$. We expect such multifractal detail to be
827 represented in the spatial distribution of alteration and mineralisation in orogenic gold
828 deposits as is indeed the case (see Chapters 6, 10 and 11). The data available to date indicate
829 that small, less endowed orogenic gold systems have relatively narrow singularity spectra for
830 gold abundances whereas larger, well-endowed deposits have wide asymmetrical singularity
831 spectra.

832 The second feature of systems exhibiting deterministic chaos is that the various states
833 of the system, although chaotic, are coupled so that not all states are possible or equally
834 probable and those that do develop define an *attractor* for that particular system. An attractor
835 is a representation of the solutions to the differential equations that describe the development
836 and evolution of the system and hence contains information on the physical and chemical
837 processes that formed the system. Some two dimensional versions of attractors are shown in
838 Figures 12.9 (d) and 12.10 (d); a three dimensional attractor is shown in Figure 12.7 (c).
839 Figure 12.14 (b) shows an attractor in (temperature – equilibrium gold solubility – gold in
840 solution) – space for the system shown in Figure 12.6. The goal for the future is to develop
841 such attractors for alteration assemblages and mineralisation in orogenic gold systems. In
842 principle, large well-endowed systems should be characterised by different attractors than
843 small, less-endowed systems.



844
845 Figure 12.14. Chaos in system behaviour. (a) Multifractal spectrum for temperature history shown in Figure 6
846 (a). (b) Attractor in (temperature - gold in solution - equilibrium gold solubility) – space for system shown in
847 Figure 8.

848 12.9. Conclusions.

849 Orogenic gold systems have been modelled as open flow thermodynamic systems in
850 which the energy balance between deformation, exothermic and endothermic mineral
851 reactions, fluid flow and heat transport is considered. The commonly observed episodic
852 behaviour characteristic of orogenic gold systems comprising mineral zoning, crack-seal vein
853 fabrics, overprinting brecciation events and multiple periods of gold deposition emerges from
854 aseismic processes operating intrinsically to the system rather than as arising from seismic
855 events extrinsic to the system. Oscillations in temperature, pore fluid pressure and the
856 equilibrium solubilities of gold, quartz and other minerals are the direct result of competition
857 between the energy and nutrients consumed by chemical reactions and the net supply of
858 energy and nutrients in the incoming and outgoing fluid streams. This intrinsic behaviour of
859 course does not rule out the influence of externally imposed adiabatic seismic events but it is
860 important to realise that orogenic gold systems with their attendant coupling between
861 chemical, hydraulic, mechanical and thermal processes are intrinsically unstable and oscillate
862 in temperature and pore pressure in non-adiabatic manners. Any external forcing by episodic
863 seismic activity can potentially couple with the intrinsic instabilities and reinforce them to
864 enhance gold deposition. It is an open question as to the relative importance of intrinsic and
865 extrinsic influences on the behaviour of orogenic gold systems. The intrinsic behaviour
866 reported here is on a much longer time scale than extrinsic seismic coupling.

867 Assuming that the incoming fluid carries gold at a concentration of a few parts per
868 billion by weight of fluid, gold grades of a few parts per million by weight of the rock can be
869 generated by the episodic partial dissolution and deposition of both the dissolved gold and the
870 incoming gold in solution over a period of 100,000 to 500,000 years. Although high
871 temperatures are important for high gold grades to develop, another critical control on the
872 gold grade for a given temperature arises from processes that increase the fluid pressure of
873 the system. These processes relate to low permeability and low thermal conductivity of the
874 country rocks. Low country rock permeability and thermal conductivity lead to higher
875 internal pore pressures and hence higher equilibrium gold solubilities and ultimately higher
876 deposited gold grades. Bonanza gold grades (ounces per tonne) in general require processes
877 that localise gold concentrations involving coupling between strongly exothermic processes
878 such as the $\text{H}_2\text{S} + \text{siderite/ankerite} \rightarrow \text{pyrite}$ reaction and the endothermic reaction:
879 $\text{gold}^{(\text{solution})} \rightarrow \text{gold}^{(\text{solid})} + \text{H}_2\text{S}$. Such coupling results in thermal solitons that sweep up
880 (remobilise) deposited gold and localise gold deposition.

881 A fundamental conclusion, commonly neglected but fundamental to targeting of high
882 grade orogenic gold deposits, is that all of the processes that lead to high gold grades can be
883 read from the energy balance of the system recorded by the paragenetic sequence and its
884 relation both spatially and temporally to deformation. Such data is readily available in drill
885 core and outcrop and becomes an important mineral exploration tool in deciding if a
886 particular deposit is likely to be of high grade.